110 μL of 13.9 M HF solution and were fed onto the chromatographic column (1.0 mm i.d. × 3.5 mm) at a flow rate of 1.2 mL min^{-1} that corresponds to 6 column volumes per second. The effluent was collected on a tantalum disk as fraction 1 and evaporated to dryness using hot helium gas and a halogen heat lamp. The remaining products in the column were stripped with 120 μL of 6.0 M HNO_3 and 0.015 M HF mixed solution at a flow rate of 1.0 mL min^{-1}. We confirmed that the above mentioned HF solution was sufficient to strip 100% of Nb and over 80% of Ta from the used anion-exchange column. The 6.0 M HNO_3/0.015 M HF effluent was collected on another tantalum disk and was evaporated to dryness as fraction 2. Both tantalum disks were automatically transferred to an α-spectrometry station equipped with eight 600 mm^2 passivated ion-implanted planar silicon (PIPS) detectors. The chromatographic separation was accomplished within 29 s and the α-particle measurement was started at 53 s and 68 s for each fraction after the collection of the products. The duration of the measurement was 238 s and 223 s for fraction 1 and 2, respectively. Spontaneous fission decay of ^{262}Db was not measured in the present study. Every step of the separation and measurement was controlled by a computer and we repeated these separation processes 1702 times with AIDA. Counting efficiencies of each detector ranged from 30–40% depending on geometrical differences of the dried sources, and the α-particle energy resolution was 100–200 keV FWHM. All events were registered event by event together with time information. After the α-particle measurement, the 221 keV γ-radiation of ^{170}Ta in every fifth pair of the samples was monitored with Ge detectors to determine the elution behavior of Ta and its chemical yield. The chemical yield of ^{170}Ta including deposition and dissolution efficiencies of the aerosols was approximately 55%.

3. Results and discussion

3.1 Batch experiments

The distribution coefficient (K_d) in units of mL g^{-1} of the atoms in question between the resin and the solution is expressed using the following equation:

$$K_d = \frac{A_r V_s}{A_s W_r}, \quad (1)$$

where A_r and A_s are the radioactivities in the resin and the solution, respectively, V_s is the volume of the acid solution (mL) and W_r the mass of the dry resin (g). In Fig. 1, the variation of the K_d values of ^{92m}Nb, ^{177}Ta, and ^{233}Pa on CA08Y is shown as a function of the initial HF concentration, $[HF]_{ini}$: log K_d vs. log $[HF]_{ini}$. The log K_d values of Nb and Ta linearly decrease with an increase of log $[HF]_{ini}$ up to around 11 M with the slopes of -2.3 ± 0.1 and -2.5 ± 0.1, respectively, while that of Pa decreases with the slope of -2.8 ± 0.1 in the studied $[HF]_{ini}$: $0.96\ M \leq [HF]_{ini} \leq 26.4\ M$. It is well known that HF is equilibrated among the following species HF, H^+, F^-, and HF_2^- in the solution and that at $[HF]_{ini} > 1$ M, the concentration of the anionic HF_2^- species is the dominant one [24]. Thus, the decrease of the log K_d values of these elements with log $[HF]_{ini}$ is interpreted as the displacement of metal fluoro complexes from the binding sites of the resin by the counter anion HF_2^-.

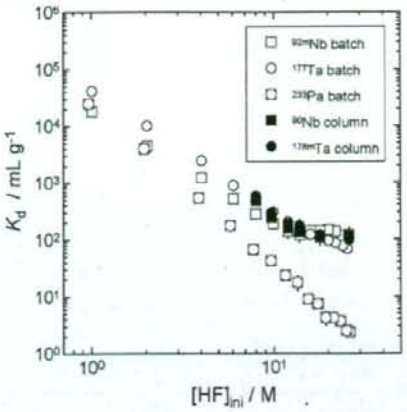

Fig. 1. Variation of the distribution coefficient, K_d, of ^{92m}Nb, ^{177}Ta, and ^{233}Pa on the anion-exchange resin CA08Y as a function of the initial HF concentration, $[HF]_{ini}$. The K_d values of ^{90}Nb and ^{178m}Ta obtained from the on-line column experiment are also shown.

Similar anion-exchange experiments with Nb, Ta, and Pa [24–31], and spectroscopic studies of Nb and Ta [32, 33] were carried out to elucidate chemical species of these elements in HF. The results show that the anionic complex of $[NbOF_5]^{2-}$ is stable at $[HF]_{ini} \leq 10$ M, while $[NbF_6]^-$ and $[NbF_7]^{2-}$ are formed at around $[HF]_{ini} > 10$ M. The sudden change of the slope for Nb in Fig. 1 suggests the transformation of the chemical species from the oxo-fluoro complex to the fluoride ones as reported by Caletka and Krivan [28]. A small change of the slope for Ta is also seen above $[HF]_{ini} \approx 15$ M. It has been reported that Ta forms in HF fluoro complexes of the form: $[TaF_6]^-$, $[TaF_7]^{2-}$, $[TaF_8]^{3-}$ and $[TaF_9]^{4-}$, and that Pa is present in the form of the anionic species of $[PaF_7]^{2-}$ and $[PaF_8]^{3-}$ in $[HF]_{ini} > 10^{-3}$ M [24–33]. Although we could not definitely identify the anionic fluoro complexes of Nb, Ta, and Pa through the present experiment, the results in Fig. 1 are consistent with those in the literature as summarized by Korkisch [34].

3.2 On-line chromatographic behavior of Nb, Ta, and Zr

In Fig. 2, typical elution curves of ^{90}Nb and ^{178m}Ta simultaneously produced in the proton-induced reactions on ^{nat}Zr and ^{nat}Hf, respectively, in 9.7, 13.9 and 26.1 M HF are depicted. According to the Glückauf formula of chromatography [35], the eluted radioactivity $A(v)$ with the effluent volume v is represented by the following equation:

$$A(v) = A_{max} \exp\left\{-\frac{N}{2}\frac{(v_p - v)^2}{v_p v}\right\}, \quad (2)$$

where parameters A_{max}, N, and v_p are the maximum peak height, the number of theoretical plates, and the peak volume, respectively. It is noted here that the v and v_p values are corrected for the dead volume (24 μL) of the present column. The results of the fit by Eq. (2) are drawn by dashed,

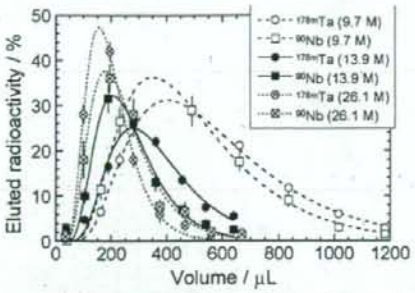

Fig. 2. Elution curves of ^{90}Nb and ^{178m}Ta in 9.7, 13.9, and 26.1 M HF at a flow rate of 1.2 mL min^{-1}. The curves indicate the results of the fits by the Glückauf equation [35].

solid, and dotted curves in Fig. 2 for each condition, showing good agreement between the experiments and the equation. The number of theoretical plates N was evaluated to be 4.5 ± 0.5. In the column chromatographic system, the K_d value is described as

$$K_d = \frac{v_p}{m_r}, \quad (3)$$

where m_r is the mass of the dry resin. The average m_r value was measured to be 1.3 ± 0.1 mg. The K_d values evaluated from the column method are also plotted in Fig. 1 and agree well with those from the static batch ones. This indicates that the anion-exchange processes taking place in the present column experiment reach equilibrium.

3.3 On-line chromatographic behavior of Db and Ta at 13.9 M HF

Based on the above batch and on-line column experiments, the chromatographic experiment of Db was conducted at $[HF]_{ini} = 13.9$ M where the K_d values of Nb/Ta are remarkably different from that of Pa. It should be interesting to observe how Db behaves on the anion-exchange resin: Nb/Ta-like or Pa-like. Further, the range of the measurable K_d values with the present AIDA system is limited by the size of the micro column (1.0 mm i.d. × 3.5 mm) to be 20 to 200. Therefore, we performed the on-line column experiment with Db at 13.9 M HF.

1702 anion-exchange experiments were conducted with AIDA. The sum of α-particle spectra of samples prepared from the two effluents, fractions 1 and 2, are shown in Fig. 3a and b, respectively. The total beam dose of ^{19}F was 2.2×10^{17} particles. The isotope ^{244}Cm, a recoil product of the target (the isotopic composition of the ^{248}Cm target is as follows: ^{244}Cm (1.12 at.%) and ^{246}Cm (1.31 at.%)), and the Fr isotopes, transfer reaction products, are mostly eluted with 13.9 M HF. As listed in Table 1, a total of 10 α events from 34-s ^{262}Db ($E_\alpha = 8.45$, 8.53 and 8.67 MeV) [36] and its daughter 3.9-s ^{258}Lr ($E_\alpha = 8.57$, 8.60, 8.62 and 8.65 MeV) [36] were registered in the energy range of 8.25–8.68 MeV, including 2 time-correlated α pairs of ^{262}Db and ^{258}Lr. The life-times of the α-decay events arising from ^{262}Db and ^{258}Lr are also listed in Table 1. The evaluated average life-time of 52.9 s resulted in a half-life of about 36.7 s that is compatible with the sum of the individual half-lives of ^{262}Db and ^{258}Lr (two of these events are ascribed

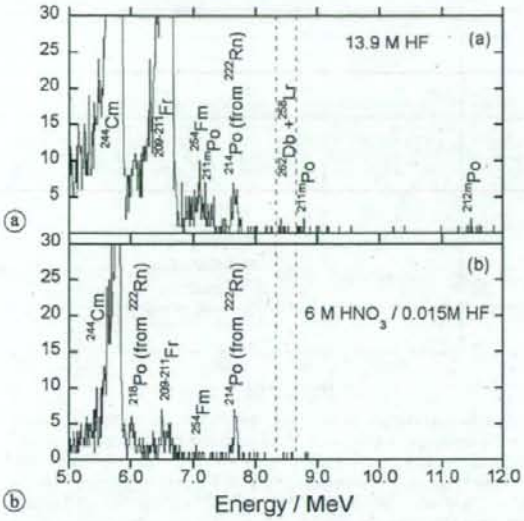

Fig. 3. Sum of α-particle spectra prepared from the two effluents: (**a**) 13.9 M HF and (**b**) 6 M HNO_3/0.015 M HF. The vertical dashed lines show the gated energy range for the analysis: 8.25–8.68 MeV.

Table 1. Observed α events in the energy range of 8.25 to 8.68 MeV.

Event No.	Fraction No.	Energy (MeV)	Life-time (s)	Remarks
1	2	8.584	71.5	
2	2	8.446	10.5	Mother
3	2	8.613	16.9	Daughter ($\Delta T = 6.4$ s)
4	1	8.449	9.4	
5	1	8.414	92.8	Mother
6	1	8.484	98.7	Daughter ($\Delta T = 5.9$ s)
7	1	8.363	142.1	
8	1	8.266	59.4	
9	1	8.382	10.1	
10	2	8.592	17.6	

to background counts as mentioned below). From the time difference ΔT between the correlated α-decay events, we obtained an average life-time of 6.2 s for the daughter nuclide ^{258}Lr.

The average background count rate from cosmic rays and electronic noise, *etc.*, was determined in a long counting interval as 3.2×10^{-6} counts s^{-1} for each detector in the α-particle energy range of interest. The total background counts resulted in 1.3 and 1.2 for fraction-1 and fraction-2, respectively. The probability of the random correlation rate was evaluated to be less than 7.4×10^{-4} during the measurement (1702×238 s and 1702×223 s for fractions 1 and 2, respectively), while the singles events subtracting the background resulted in 7.5. The event ratio between the total α counts and α–α correlations was estimated to be 10 : 1.7, taking into consideration the counting efficiency of the detector (35%), the recoil effect of ^{258}Lr, and the decay of ^{262}Db and ^{258}Lr. The observed ratio of 7.5 : 2 is reasonably consistent with the estimated one within the counting statis-

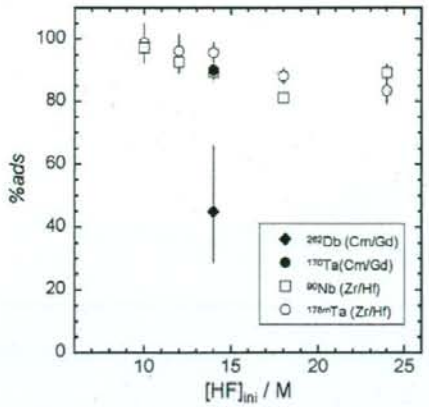

Fig. 4. Variation of the adsorption probability, % ads, of Nb, Ta, and Db on the anion-exchange resin CA08Y obtained from the on-line column experiments as a function of the initial HF concentration, $[HF]_{ini}$. The data of ^{262}Db and ^{170}Ta obtained from the Cm/Gd target are shown by closed symbols, while those of ^{90}Nb and ^{178m}Ta from the Zr/Hf targets are shown by open ones.

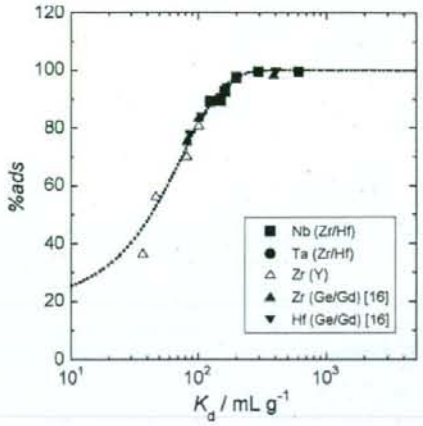

Fig. 5. Variation of the adsorption probability, % ads, of Nb and Ta produced from the Zr/Hf targets on the anion-exchange resin CA08Y as a function of the distribution coefficient, K_d. The data of Zr produced from ^{89}Y(p, n) are depicted by open triangles. The % ads values of Zr and Hf produced from the Ge/Gd targets taken from [16] are shown by closed triangles and inverse triangles, respectively.

tics. The evaluated production cross section of ^{262}Db based on the total α-events of 7.5 was about 1 nb by assuming the α-decay branch of $I_\alpha = 64\%$ in ^{262}Db [36] that is consistent with the previous value in [23].

From the radioactivities A_1 and A_2 measured in fractions 1 and 2, respectively, the adsorption probability (% ads) on CA08Y was evaluated using the relation: $\%\,\text{ads} = 100A_2/(A_1 + A_2)$. The corrections for the radioactive decay and the background were considered for A_1 and A_2. Because of the short half-life of ^{258}Lr, the contribution of ^{258}Lr formed from ^{262}Db during the collection before the chemical separation was not taken into account. The % ads values of ^{262}Db and ^{170}Ta were 45^{+21}_{-16}% and 90 ± 2%, respectively, as shown in Fig. 4. The error limits of the % ads value of ^{262}Db was evaluated from the counting statistics of the observed α events based on the 68% confidence intervals for Poisson distributed variables [37]. The % ads values of ^{90}Nb and ^{178m}Ta produced from the Zr/Hf target in the separate run are also depicted in Fig. 4 as a function of $[HF]_{ini}$. It should be noted here that the data of Ta from both runs are in good agreement. It is clearly seen that the % ads value of Db is much smaller than those of Nb and Ta.

The K_d value of Db was evaluated by assuming that the kinetics in the complexation and ion-exchange processes of Db is as fast as those for the homologues as described in [16, 17]. In Fig. 5, the correlation between the % ads and K_d values of Nb and Ta are plotted together with the data of Zr produced in ^{89}Y(p, n) and those of Zr and Hf taken from [16]. The % ads values of those elements are found to be smoothly correlated with K_d,

$$\%\,\text{ads} = 100 \exp\left[-a \exp\left\{-b(K_d - c)\right\}\right]. \quad (4)$$

The % ads value of Db from the column method can be transformed into the K_d value using Eq. (4). The obtained K_d is shown in Fig. 6 together with those of Nb, Ta, and Pa obtained from the batch experiment. The K_d values of the group-4 elements, Zr, Hf, and Rf taken from Ref. [16], are

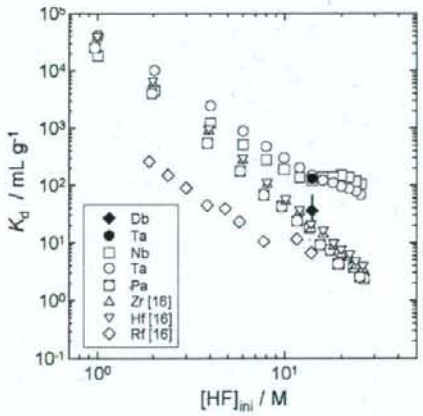

Fig. 6. Variation of the distribution coefficient, K_d, of Db, Nb, Ta, and Pa on the anion-exchange resin CA08Y as a function of $[HF]_{ini}$. The values of Db and Ta obtained from the on-line column experiment are indicated by closed symbols, while those of Nb, Ta and Pa obtained from the batch experiment are shown by open symbols. The K_d values of Rf, Zr and Hf taken from Ref. [16] are also plotted.

also plotted. The errors associated with ^{262}Db are propagated from the error limits of the % ads value. As seen from Fig. 6, the K_d value of Db is significantly smaller than those of Nb and Ta at $[HF]_{ini} = 13.9$ M, while it is larger than that of Pa. The result demonstrates that the adsorption of these elements is in the sequence of Ta $\approx$ Nb > Db $\geq$ Pa. The present result is not contradictory to that in the amine extraction study of Db at 4 M HF [12]. The lower limit value of K_d in [12] would be beyond the limit of measurable K_d values with the micro columns.

As shown in Fig. 6 and described in [14–19], it has been found that the fluoride complexation of Rf is significantly weaker than that of Zr and Hf, but it is stronger than

the complexation of Th. The present result ascertains that a similar tendency is observed also in the group-5 elements. According to theoretical calculations [38], the order of the complex formation of $[MF_6]^-$ (M = Nb, Ta, Db, and Pa) is predicted to be Pa $\gg$ Nb > Db > Ta that is defined by a predominant electrostatic energy of the metal–ligand interaction. In the present case, however, chemical forms of the group-5 elements are not determined as mentioned, although some species are reported to be presumably $[MF_6]^-$, $[MF_7]^{2-}$, and/or $[MF_8]^{3-}$ in 13.9 M HF. Thus, we have to determine the chemical forms of these elements to compare the experimental adsorption sequence with that from predictions.

4. Conclusions

The distribution coefficients of Db and its lighter homologues of the group-5 elements Nb and Ta, and the pseudo-homologue Pa were measured by anion-exchange chromatography. It was found that the adsorption of Db on the anion-exchange resin was evidently smaller than those of Nb and Ta, while it was larger than that of Pa: Ta $\approx$ Nb > Db $\geq$ Pa at 13.9 M HF.

Acknowledgment. The authors express their gratitude to the crew of the JAEA tandem accelerator for their invaluable assistance in the course of these experiments. This work was supported in part by the JAEA-University Collaboration Research Project and the Program on the Scientific Cooperation between JAEA and GSI in Research and Development in the Field of Ion Beam Application.

References

1. Schädel, M. (ed.): *The Chemistry of Superheavy Elements*. Kluwer Academic Publishers, Dordrecht (2003).
2. Kratz, J. V.: Critical evaluation of the chemical properties of the transactinide elements. Pure Appl. Chem. **75**, 103 (2003).
3. Kratz, J. V.: Chemistry of Transactinides. In: *Handbook of Nuclear Chemistry*. Vol. 2 (Vértes, A., Nagy, S., Klencsár, Z., eds.) Kluwer Academic Publishers, Dordrecht (2003), p. 323.
4. Schädel, M.: Chemistry of superheavy elements. Angew. Chem. Int. Ed. **45**, 368 (2006).
5. Hoffman, D. C., Lee, D. M., Pershina, V.: Transactinide elements and future elements. In: *The Chemistry of the Actinides and Transactinide Elements*. 3rd Edn., Vol. 3 (Morss, L. R., Edelstein, N. M., Fuger, J., eds.) Springer, Dordrecht (2006), p. 1652.
6. Eichler, R., Aksenov, N. V., Belozerov, A. V., Bozhikov, G. A., Chepigin, V. I., Dmitriev, S. N., Dressler, R., Gäggeler, H. W., Gorshkov, V. A., Haenssler, F., Itkis, M. G., Laube, A., Lebedev, V. Ya., Malyshev, O. N., Oganessian, Yu. Ts., Petrushkin, O. V., Piguet, D., Rasmussen, P., Shishkin, S. V., Shutov, A. V., Svirikhin, A. I., Tereshatov, E. E., Vostokin, G. K., Wegrzecki, M., Yeremin, A. V.: Chemical characterization of element 112. Nature **447**, 72 (2007).
7. Gregorich, K. E., Henderson, R. A., Lee, D. M., Nurmia, M. J., Chasteler, R. M., Hall, H. L., Bennett, D. A., Gannett, C. M., Chadwick, R. B., Leyba, J. D., Hoffman, D. C., Herrmann, G.: Aqueous chemistry of element 105. Radiochim. Acta **43**, 223 (1988).
8. Kratz, J. V., Zimmermann, H. P., Scherer, U. W., Schädel, M., Brüchle, W., Gregorich, K. E., Gannett, C. M., Hall, H. L., Henderson, R. A., Lee, D. M., Leyba, J. D., Nurmia, M. J., Hoffman, D. C., Gäggeler, H., Jost, D., Baltensperger, U., Ya Nai-Qi, Türler, A., Lienert, Ch.: Chemical properties of element 105 in aqueous solution: Halide complex formation and anion exchange into triisooctyl amine. Radiochim. Acta **48**, 121 (1989).
9. Gober, M. K., Kratz, J. V., Zimmermann, H. P., Schädel, M., Brüchle, W., Schimpf, E., Gregorich, K. E., Türler, A., Hannink, N. J., Czerwinski, K. R., Kadkhodayan, B., Lee, D. M., Nurmia, M. J., Hoffman, D. C., Gäggeler, H., Jost, D., Kovács, J., Scherer, U. W., Weber, A.: Chemical properties of element 105 in aqueous solution: Extractions into diisobutylcarbinol. Radiochim. Acta **57**, 77 (1992).
10. Schädel, M., Brüchle, W., Schimpf, E., Zimmermann, H. P., Gober, M. K., Krtaz, J. V., Trautmann, N., Gäggeler, H., Jost, D., Kovács, J., Scherer, U. W., Weber, A., Gregorich, K. E., Türler, A., Czerwinski, K. R., Hannink, N. J., Kadkhodayan, B., Lee, D. M., Nurmia, M. J., Hoffman, D. C.: Chemical properties of element 105 in aqueous solution: Cation exchange separation with α-hydroxyisobutyric acid. Radiochim. Acta **57**, 85 (1992).
11. Zimmermann, H. P., Gober, M. K., Kratz, J. V., Schädel, M., Brüchle, W., Schimpf, E., Gregorich, K. E., Türler, A., Czerwinski, K. R., Hannink, N. J., Kadkhodayan, B., Lee, D. M., Nurmia, M. J., Hoffman, D. C., Gäggeler, H., Jost, D., Kovács, J. Scherer, U. W., Weber, A.: Chemical properties of element 105 in aqueous solution: back extraction from triisooctyl amine into 0.5 M HCl. Radiochim. Acta **60**, 11 (1993).
12. Paulus, W., Kratz, L. V., Strub, E., Zauner, S., Brüchle, W., Pershina, V., Schädel, M., Schausten, B., Adams, J. L., Gregorich, K. E., Hoffman, D. C., Lane, M. R., Laue, C., Lee, D. M., McGrath, C. A., Shaughnessy, D. K., Strellis, D. A., Sylwester, E. R.: Chemical properties of element 105 in aqueous solution: extraction of the fluoride-, chloride-, and bromide complexes of the group-5 elements into an aliphatic amine. Radiochim. Acta. **84**, 69 (1999).
13. Trubert, D., Naour, C. Le, Guzman, F. M., Hussonnois, M., Brillard, L., Le Du, J. F., Constantinescu, O., Gasparro, J., Barci, V., Weiss, B., Ardisson, G.: Chemical isolation of dubnium (element 105) in fluoride media. Radiochim. Acta **90**, 127 (2002).
14. Strub, E., Kratz, J. V., Kronenberg, A., Nähler, A., Thörle, P., Zauner, S., Brüchle, W., Jäger, E., Schädel, M., Schausten, B., Schimpf, E., Zongwei, Li, Kirbach, U., Schumann, D., Jost, D., Türler, A., Asai, M., Nagame, Y., Sakama, M., Tsukada, K., Gäggeler, H. W., Glatz, J. P.: Fluoride complexation of rutherfordium (Rf, Element 104). Radiochim. Acta **88**, 265 (2000).
15. Kronenberg, A., Eberhardt, K., Kratz, J. V., Mohapatra, P. K., Nähler, A., Thörle, P., Brüchle, W., Schädel, M., Türler, A.: On-line anion exchange of rutherfordium in HF/HNO_3 and HF solutions. Radiochim. Acta **92**, 379 (2004).
16. Haba, H., Tsukada, K., Asai, M., Toyoshima, A., Akiyama, K., Nishinaka, I., Hirata, M., Yaita, T., Ichikawa, S., Nagame, Y., Yasuda, K., Miyamoto, Y., Kaneko, T., Goto, S., Ono, S., Hirai, T., Kudo, H., Shigekawa, M., Shinohara, A., Oura, Y., Nakahara, H., Sueki, K., Kikunaga, H., Kinoshita, N., Tsuruga, N., Yokoyama, A., Sakama, M., Enomoto, S., Schädel, M., Brüchle, W., Kratz, J. V.: Fluoride complexation of element 104, rutherfordium. J. Am. Chem. Soc. **126**, 5219 (2004).
17. Toyoshima, A., Haba, H., Tsukada, K., Asai, M., Akiyama, K., Nishinaka, I., Nagame, Y., Saika, D., Matsuo, K., Sato, W., Shinohara, A., Ishizu, H., Ito, M., Saito, J., Goto, S., Kudo, H., Kikunaga, H., Kinoshita, N., Kato, C., Yokoyama, A., Sueki, K.: Elution curve of rutherfordium (Rf) in anion-exchange chromatography with hydrofluoric acid (HF) solution. J. Nucl. Radiochem. Sci. **5**, 45 (2004).
18. Toyoshima, A., Haba, H., Tsukada, K., Asai, M., Akiyama, K., Goto, S., Sato, W., Ishii, Y., Nishinaka, I., Sato, T. K., Nagame, Y., Tani, Y., Hasegawa, H., Matsuo, K., Saika, D., Kitamoto, Y., Shinohara, A., Ito, M., Saito, J., Kudo, H., Yokoyama, A., Sakama, M., Sueki, K., Oura, Y., Nakahara, H., Schädel, M., Brüchle, W., Kratz, J. V.: Hexafluoro complex of rutherfordium in mixed HF/HNO_3 solutions. Radiochim. Acta **96**, 125 (2008).
19. Ishii, Y., Toyoshima, A., Tsukada, K., Asai, M., Toume, H., Nishinaka, I., Nagame, Y., Miyashita, S., Mori, S., Suganuma, H., Haba, H., Sakamaki, M., Goto, S., Kudo, H., Akiyama, K., Oura, Y., Nakahara, H., Tashiro, Y., Shinohara, A., Schädel, M., Brüchle, W., Pershina, V., Kratz, J. V.: Fluoride complexation of element 104, rutherfordium (Rf), investigated by cation-exchange chromatography. Chem. Lett. **37**, 288 (2008).
20. Nagame, Y., Tsukada, K., Asai, M., Toyoshima, A., Akiyama, K., Ishii, Y., Kaneko-Sato, T., Hirata, M., Nishinaka, I., Ichikawa, S., Haba, H., Enomoto, S., Matsuo, K., Saika, D., Kitamoto, Y., Hasegawa, H., Tani, Y., Sato, W., Shinohara, A., Ito, M., Saito, J., Goto, S., Kudo, H., Kikunaga, H., Kinoshita, N., Yokoyama, A., Sueki, K., Oura, Y., Nakahara, H., Sakama, M., Schädel, M.,

Brüchle, W., Kratz, J. V.: Chemical studies on rutherfordium (Rf) at JAERI. Radiochim. Acta **93**, 519 (2005).
21. Kasamatsu, Y., Toyoshima, A., Toume, H., Tsukada, K., Haba, H., Nagame, Y.: Anion-exchange behavior of Nb, Ta, and Pa as homologues of Db in HF/HNO_3 solutions. J. Nucl. Radiochem. Sci. **8**, 69 (2007).
22. Schädel, M., Brüchle, W., Jäger, E., Schimpf, E., Kratz, J. V., Scherer, U. W., Zimmermann, H. P.: ARCA-II – a new apparatus for fast, repetitiveve HPLC separation. Radiochim. Acta **48**, 171 (1989).
23. Nagame, Y., Asai, M., Haba, H., Goto, S., Tsukada, K., Nishinaka, I., Nishio, K., Ichikawa, S., Sakama, M., Toyoshima, A., Akiyama, K., Nakahara, H., Schädel, M., Kratz, J. V., Gäggeler, H. W., Türler, A.: Production cross sections of ^{261}Rf and ^{262}Db in bombardments of ^{248}Cm with ^{18}O and ^{19}F ions. J. Nucl. Radiochem. Sci. **3**, 85 (2002), private communication.
24. Plaisance, M., Guillaumont, R.: Fluoro- et chlorofluoro-complexes de protactinium pentavalent. Radiochim. Acta **12**, 32 (1969).
25. Varga, L. P., Freund, H.: The formation constants of the tantalum fluoride system. I. Potentiometric and anion exchange studies – Evidence for species of coordination number nine. J. Phys. Chem. **66**, 21 (1962).
26. Keller, C.: Untersuchungen über das Verhalten von Niob, Tantal und Protactinium gegenüber Ionenaustauschern. Radiochim. Acta **1**, 147 (1963).
27. Kim, J. L., Lagally, H., Born, H.-J.: Ion exchange in aqueous and in aqueous-organic solvents. Part I. Anion-exchange behavior of Zr, Nb, Ta and Pa in aqueous HCl-HF and in HCl-organic solvent. Anal. Chim. Acta **64**, 29 (1973).
28. Caletka, R., Krivan, V.: Behavior of 18 elements in HF and HF-NH_4F media on anion exchanger in various ionic forms. J. Radioanal. Nucl. Chem. **142**, 359 (1990).
29. Monroy-Guzman, F., Trubert, D., Brillard, L., Kim, J. B., Hussonnois, M., Constantinescu, O.: Adsorption of Zr, Hf, Nb, Ta and Pa on macroporous anion exchangers in HF medium. J. Radioanal. Nucl. Chem. **208**, 461 (1996).
30. Trubert, D., Monroy-Guzman, F., Le Naour, C., Brillard, L., Hussonnois, M., Constantinescu, O.: Behaviour of Zr, Hf, Nb, Ta and Pa on macroporous anion exchangers in chloride-fluoride media. Anal. Chim. Acta **374**, 149 (1998).
31. Myasoedov, B. F., Kirby, H. W., Tananaev, I. G.: Protactinium. In: *The Chemistry of the Actinides and Transactinide Elements*. 3rd Edn., Vol. 1 (Morss, L. R., Edelstein, N. M., Fuger, J., eds.), Springer, Dordrecht (2006), p. 161.
32. Keller Jr., O. L.: Identification of complex ions of niobium (V) in hydrofluoric acid solution by Raman and infrared spectroscopy. Inorg. Chem. **2**, 783 (1963).
33. Keller Jr., O. L., Chetham-Strode Jr., A.: A study by Raman spectroscopy of complex ions formed by tantalum (V) in the system Ta(V)-HF-NH_4F-H_2O. Inorg. Chem. **5**, 367 (1966).
34. Korkisch, J.: *Handbook of Ion Exchange Resins: Their Application to Inorganic and Analytical Chemistry*. CRC Press, Florida (1989).
35. Glückauf, E.: Theory of chromatography. Part 9. The "theoretical plate" concept in column separations. Trans. Faraday Soc. **51**, 34 (1955).
36. Firestone, R. B., Shirley, V. S.: *Table of Isotopes*. 8th Edn., John Wiley and Sons, New York (1996).
37. Brüchle, W.: Confidénce intervals for experiments with background and small numbers of events. Radiochim. Acta **91**, 71 (2003).
38. Pershina, V., Bastug, T.: Solution chemistry of element 105 Part III: Hydrolysis and complex formation of Nb, Ta, Db and Pa in HF and HBr solutions. Radiochim. Acta **84**, 79 (1999).

DOI: 10.1007/s10967-007-7320-6 Journal of Radioanalytical and Nuclear Chemistry, Vol. 279, No.2 (2009) 371–376

Adsorption of Nb, Ta and Pa on anion-exchanger in HF and HF/HNO_3 solutions: Model experiments for the chemical study of Db

Y. Kasamatsu,[1]* A. Toyoshima,[1] H. Haba,[2] H. Toume,[1] K. Tsukada,[1] K. Akiyama,[3] T. Yoshimura,[4] Y. Nagame[1]

[1] Advanced Science Research Center, Japan Atomic Energy Agency, Tokai, Ibaraki 319-1195, Japan
[2] Nishina Center for Accelerator Based Science, RIKEN, Wako, Saitama 351-0198, Japan
[3] Graduate School of Science and Engineering, Tokyo Metropolitan University, Hachioji, Tokyo 192-0397, Japan
[4] Graduate School of Science, Osaka University, Toyonaka, Osaka 560-0043, Japan

(Received March 10, 2008)

Anion-exchange behavior of the group-5 elements, Nb and Ta, and their pseudo homologue Pa in HF and HF/HNO_3 solutions was investigated by a batch method to find suitable conditions for the anion-exchange experiment of element 105 (Dubnium, Db). We determined the distribution coefficients of those elements on the anion-exchange resin as a function of the F^- and NO_3^- concentrations. Clearly different anion-exchange behavior was observed among these elements. Based on the results, we discuss the fluoro-complex formation of each element and suggest experimental conditions for the study of fluoride complexation of Db.

Introduction

The transactinide elements with atomic numbers $Z \geq 104$ must be produced by accelerators using nuclear reactions of heavy-ion beams with heavy target materials. Chemical studies of such elements are conducted on a one-atom-at-a-time basis by rapid chemical separation techniques because of considerably low production rates and short half-lives of the transactinide nuclides.[1,2] Chemical experiments of the transactinide elements are often performed together with their lighter homologues to compare the properties with those of the homologues.

Several model experiments aiming at the chemical study of Dubnium (Db) in aqueous solution have been performed using the lighter homologues Nb and Ta, and the pseudo homologue Pa.[3–6] Some mutual separations of the group-5 homologues by chromatographic methods have been applied to the isolation of ^{262}Db ($T_{1/2}$ = 34 s) and ^{263}Db ($T_{1/2}$ = 27 s) produced in proper nuclear reactions, and the behavior of Db was compared with that of the homologues under each experimental condition.[7–14] For clear understanding of the chemical properties of Db, further systematic investigations are strongly required.

Chemical characterization of Db is also important to verify the synthesis of element 115.[15,16] A long-lived spontaneously fissioning nuclide which is one of the descendants of ^{288}Db (Z = 115) produced in the ^{243}Am(^{48}Ca, 3n) reaction was assigned to ^{268}Db or, after EC-decay, to ^{268}Rf (Z = 104).[16] To confirm the above assignment, the long-lived nuclides ^{268}Db/^{268}Rf have to be unequivocally identified by definite chemical isolations of Db and Rf; the chemical behavior of these elements should be established.

In our previous works, distribution coefficients (K_d) of Rf were successfully determined by the anion-exchange experiments in HF and HF/HNO_3 solutions with AIDA (Automated Ion-exchange separation apparatus coupled with the Detection system for Alpha-spectroscopy), and the results clearly showed that the fluoride complexation of Rf is significantly weaker than that of the homologues Zr and Hf.[17–19] Quite unique and unexpected behavior of Rf was observed in the fluoride complexation. As a subsequent step, we plan to investigate fluoride complexation of Db through anion-exchange experiments in HF/HNO_3; the K_d values of Db will be systematically measured as a function of the ligand (F^-) and the counter-ion (NO_3^-) concentrations as those with Rf.[18] The K_d values of Nb, Ta and Pa on the anion-exchange resin were previously determined as a function of the fluoride ion concentration ([F^-]) in HF/HNO_3 at [NO_3^-] = 0.1M.[20] In this work, variations of the K_d values of these elements were accurately measured as a function of [NO_3^-] for further discussion on the formation of anionic fluoro complexes of the group-5 elements. Based on the results, we propose suitable experimental conditions for the anion-exchange chromatography of Db.

Experimental

We used the radiotracers of ^{95}Nb, ^{177,179}Ta and ^{233}Pa to measure the K_d values on the anion-exchange resin. The experimental procedures are basically the same as those described in the previous report.[20]

* E-mail: kasamatsu.yoshitaka@jaea.go.jp

0236–5731/USD 20.00

Akadémiai Kiadó, Budapest
Springer, Dordrecht

The K_d value is obtained from a ratio of the radioactivity in the resin phase (A_r) to that in the solution (A_s) as:

$$K_d = \frac{A_r V_s}{A_s W_r} \quad (1)$$

where V_s is the volume of the solution (mL) and W_r the weight of the dry resin (g). In a polypropylene (PP) test tube, 8–200 mg of the dried anion-exchange resin MCI GEL CA08Y (particle size of 25 μm) and 3 mL of HF or HF/HNO_3 solution containing the radiotracers of ^{95}Nb, $^{177,179}Ta$ and ^{233}Pa were mixed. In each sample, the numbers of atoms of the radiotracers were 10^8–10^{12}. Then, the tube was shaken for 15 minutes. After centrifugation, 1 mL of the solution was pipetted into a small PP container and subjected to X- and γ-ray spectrometry with a Ge semiconductor detector. The same treatment was conducted without resin to monitor the reference radioactivity in each solution. The radioactivity in the resin phase was evaluated by subtracting that in the supernatant solution from the reference radioactivity. Only statistical errors were taken into account for the evaluation of errors in the K_d values. The K_d values of Nb, Ta and Pa on the anion-exchange resin in HF/HNO_3 solutions were determined as a function of $[NO_3^-]$ under the following conditions: the constant fluoride ion concentration $[F^-]=2.0\cdot10^{-4}$, $3.0\cdot10^{-3}$ and $1.0\cdot10^{-2}$ M. The K_d values in pure HF solutions ($[NO_3^-]=0$M) were also measured as a function of $[F^-]$ in the concentration range of $8.9\cdot10^{-3}$–$1.7\cdot10^{-2}$M (0.11–2.0M HF). The fluoride ion concentrations were calculated using the dissociation constants of HF and HF_2^- for equilibria expressed by the following chemical reactions (2) and (3), respectively:[21]

$$H^+ + F^- \rightleftarrows HF \quad (2)$$

$$HF + F^- \rightleftarrows HF_2^- \quad (3)$$

Results and discussion

Variations of the K_d values of Nb, Ta and Pa on the anion-exchange resin in HF/HNO_3 solutions are shown in Fig. 1 as a function of $[NO_3^-]$ at constant $[F^-]$ of (a) $2.0\cdot10^{-4}$, (b) $3.0\cdot10^{-3}$ and (c) $1.0\cdot10^{-2}$M. In the $\log K_d$ vs. $\log[NO_3^-]$ plot, $\log K_d$ linearly decreases with increasing $\log[NO_3^-]$ for every element. Thus, we fitted a linear expression to the data with the least squares fitting. The slopes of the fitted lines are presented in Table 1. In every concentration of $[F^-]$, the absolute values of the minus slopes are in the sequence of Pa>Nb>Ta. The present K_d values at $[NO_3^-]=0.1$M are in good agreement with those obtained in the previous study as depicted in Fig. 2. The K_d values obtained in HF solutions are also plotted in Fig. 2. It is obvious from the figure that the K_d values of the elements become small in HF/HNO_3 by the effect of the NO_3^- ions as a counter ion and that the differential between the K_d values in HF and those in HF/HNO_3 is the largest for Pa, which is consistent with the largest absolute value of the slope for Pa in Table 1.

On the assumption that consecutive coordination of the fluoride ion to metal cations proceeds in the formation of the anionic fluoro complexes or oxo-fluoro complexes with increasing $[F^-]$,[20] formation constants of the anionic complexes with –1 and –2 charges are given by:

$$K_6 = \frac{[MF_6^-]}{[MF_5][F^-]} \quad (4)$$

and

$$K_7 = \frac{[MF_7^{2-}]}{[MF_6^-][F^-]} \quad (5)$$

respectively, where M represents the pentavalent metal ion as M^{5+}. In the case of the oxo-fluoro complexes, MO^{3+} is substituted for MF_2^{3+}; for example, the complex MOF_4^- is replaced by MF_6^-.

Equilibrium constants of anion-exchange reactions, D_6 and D_7, with the resin are expressed by:

$$D_6 = \frac{[RMF_6][L^-]}{[MF_6^-][RL]} \quad (6)$$

$$D_7 = \frac{[R_2MF_7][L^-]^2}{[MF_7^{2-}][RL]^2} \quad (7)$$

where R and L^- represent the anion-exchange resin and a counter ion, respectively. Formation of the complex with a –3 charge and further charged anionic complexes are not taken into consideration because the complexes with the –1 and/or –2 charges are the dominant species in both the solution and the resin phase even in concentrated HF solutions for Nb and Ta, which has been verified from the EXAFS and Raman spectroscopic studies of these elements.[22,23]

Table 1. Slopes (s) of the fitted linear lines in Fig. 1: $\log K_d = s \log [NO_3^-] + C$

$[F^-]$, M	Slope (s)		
	Nb	Ta	Pa
$2.0\cdot10^{-4}$	-1.0 ± 0.1	-0.5 ± 0.1	-1.2 ± 0.1
$3.0\cdot10^{-3}$	-1.3 ± 0.1	-1.2 ± 0.1	-1.8 ± 0.1
$1.0\cdot10^{-2}$	-1.5 ± 0.1	-1.3 ± 0.1	-2.0 ± 0.1

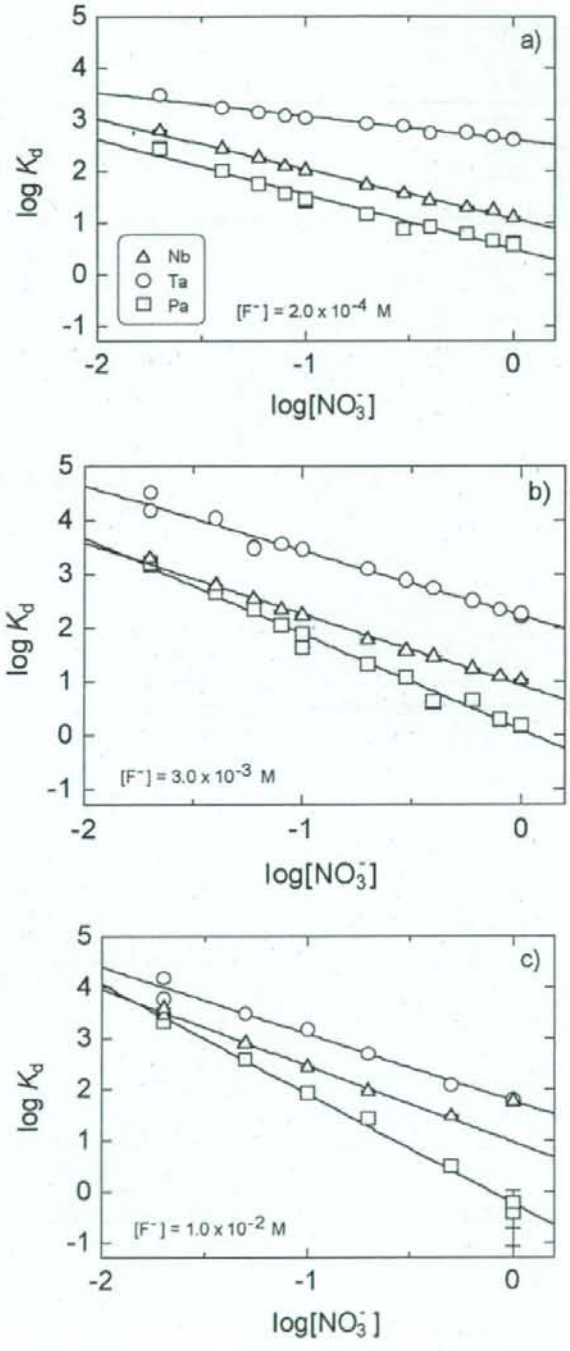

Fig. 1. Variations of the K_d values of ^{95}Nb, ^{179}Ta and ^{233}Pa on the anion-exchange resin as a function of $[NO_3^-]$ at the constant $[F^-]$ of (a) $2.0 \cdot 10^{-4}$, (b) $3.0 \cdot 10^{-3}$ and (c) $1.0 \cdot 10^{-2}$M

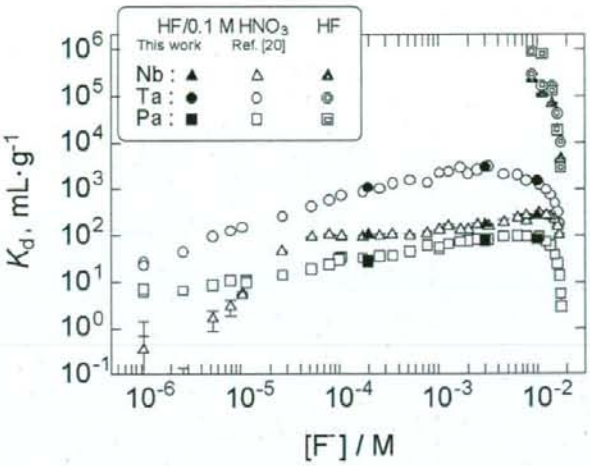

Fig. 2. Variations of the K_d values of Nb, Ta and Pa on the anion-exchange resin as a function of [F$^-$] in HF/HNO_3 media (closed symbols) and in HF media (twofold symbols) together with those reported in Reference 20 (open symbols)

It is also reported that Pa forms the anionic fluoro complexes of PaF_6^- and/or PaF_7^{2-} except in the extremely concentrated HF solution.[24–26] The K_d values in the exchange reaction of the complexes of interest between the solution and the resin phase is described as:

$$K_d = \frac{[RMF_6]+[R_2MF_7]}{[MF_5]+[MF_6^-]+[MF_7^{2-}]} \quad (8)$$

From Eqs (4) to (7), the following expression is obtained:

$$K_d = \frac{[RL][L^-]K_6D_6[F^-]+[RL]^2K_6K_7D_7[F^-]^2}{[L^-]^2(1+K_6[F^-]+K_6K_7[F^-]^2)} \quad (9)$$

When only single species dominantly interacts with the resin, Eqs (10) and (11) are given for the species with the –1 and –2 charges, respectively:

$$\log K_d = -\log\frac{[L^-]}{[RL]} + \log K_6D_6 + \log\left(\frac{[F^-]}{1+K_6[F^-]+K_6K_7[F^-]^2}\right) \quad (10)$$

$$\log K_d = -2\log\frac{[L^-]}{[RL]} + \log K_6K_7D_7 + \log\left(\frac{[F^-]^2}{1+K_6[F^-]+K_6K_7[F^-]^2}\right) \quad (11)$$

The concentration of the counter ion in the resin phase, [RL], can be regarded as a constant value because it is equal to the exchange capacity of the resin phase. Since the contribution of F^- and HF_2^- as the counter ions is negligible at [F$^-$]<5·10^{-3}M in HF/HNO_3 solutions,[18] [L$^-$] can be replaced by [NO_3^-] in such [F$^-$] range. Thus, the slope of the linear fit in the logK_d vs. log[NO_3^-] plot at constant [F$^-$] of <5·10^{-3}M corresponds to the charge of the anionic complex which interacts with the resin. In this work, therefore, the charges of the complexes can be evaluated from the slopes under the following conditions, [F$^-$]=2.0·10^{-4} and 3.0·10^{-3}M (Figs 1a and 1b). The relationship between the slope and the electric charge of the complex ion holds even if the existences of the metal cation (M^{5+}) and other fluoro complexes such as MF^{4+} and MF_2^{3+} in the solution are taken into account.[18]

The absolute value of the minus slope in Table 1 becomes larger for every element with increasing [F$^-$]. This means that the coordination number of the fluoride ion to the metal cation increases with increasing [F$^-$], indicating the consecutive formation of the fluoro complexes of the group-5 elements. The sequence of the absolute slope values for the elements mentioned above (Pa>Nb>Ta) corresponds to that of the charge number of the anionic complexes on the condition that [F$^-$]=2.0·10^{-4} and 3.0·10^{-3}M.

As for chemical species, it is reported that Ta and Pa form fluoro complexes MF_n^{5-n}, while Nb is dominantly present as oxo-fluoro complexes $NbOF_n^{3-n}$ in aqueous solutions containing fluoride ions with a wide range of [F$^-$].[4–6,22–27] Especially, the EXAFS and Raman spectroscopic studies of Nb and Ta suggest that TaF_7^{2-} and $NbOF_5^{2-}$ are the dominant species in 0.1–10M HF solutions ([F$^-$]=8.9·10^{-3}–1.9·10^{-2}M).[22,23]

From the present results, it is deduced that Nb forms the anionic complex $NbOF_4^-$ which interacts with the anion-exchange resin at the diluted $[F^-]$, whereas $NbOF_5^{2-}$ would coexists at $[F^-]=3.0\cdot10^{-3}$M. Tantalum would form the TaF_6^- complex at $[F^-]$ of $3.0\cdot10^{-3}$M. From the slope of –0.5 at $[F^-]=2.0\cdot10^{-4}$M in Table 1, it would be possible to interpret that hydrolysis species of Ta are present at such dilute F^- concentration. Actually hydrolysis species is reported to dominate the fluoride complexation of Ta at $[F^-]$ lower than $1\cdot10^{-3}$M.[5] PaF_6^- and PaF_7^{2-} are considered to be formed at $[F^-]$ of $2.0\cdot10^{-4}$ and $3.0\cdot10^{-3}$M, respectively.

Regardless of the clear difference in chemical species between Nb and Ta, the variations of the K_d values of Nb and Ta as a function of $[F^-]$ as well as the absolute values of the K_d values are quite similar with each other in HF solutions under the studied conditions as shown in Fig. 2. On the other hand, in HF/HNO_3, the K_d values of Nb are quite different from those of Ta, and a unique variation of the K_d values of Nb against $[F^-]$ is observed,[20] probably reflecting its uniqueness of the chemical species. To discuss the fluoride complexation of the group-5 elements including Db, a systematic anion-exchange study of Db in HF/HNO_3 is indispensable. The K_d values of Db should be determined in a wide range of $[F^-]$ to observe consecutive formation of the fluoro complexes. The variation of the K_d values as a function of $[NO_3^-]$ should be also measured in the concentration range of $[F^-]<5\cdot10^{-3}$M to evaluate the charge number of the complex of Db without the influence of the other counter ions.

Conclusions

The K_d values of Nb, Ta and Pa on the anion-exchange resin were determined as a function of $[NO_3^-]$, and clearly different anion-exchange behavior was observed among the elements in HF/HNO_3 solutions. Analysis of the slopes of the linear fittings in the $\log K_d$ vs. $\log[NO_3^-]$ plot enables us to evaluate the charges of the anionic fluoro complexes of the group-5 elements. Their chemical species were deduced based on the knowledge in the references as follows: (1) $NbOF_4^-$ would be present at $[F^-]=2.0\cdot10^{-4}$ and $3.0\cdot10^{-3}$M, (2) TaF_6^- seems to be dominantly present at $[F^-]=3\cdot10^{-3}$M and Ta is hydrolyzed at $[F^-]=2.0\cdot10^{-4}$M, and (3) PaF_6^- and PaF_7^{2-} would be dominantly present at $[F^-]=2.0\cdot10^{-4}$ and $3.0\cdot10^{-3}$M, respectively.

*

The authors thank the staffs of the RIKEN Accelerator Research Facility for the productions of ^{95}Nb and ^{179}Ta.

References

1. M. SCHÄDEL, Angew. Chem. Intern. Ed., 45 (2006) 368.
2. J. V. KRATZ, Pure Appl. Chem., 75 (2003) 103.
3. M. SCHÄDEL, W. BRÜCHLE, E. JÄGER, E. SCHIMPF, J. V. KRATZ, U. W. SCHERER, H. P. ZIMMERMANN, Radiochim. Acta, 48 (1989) 171.
4. F. MONROY GUZMAN, D. TRUBERT, L. BRILLARD, J. B. KIM, M. HUSSONNOIS, O. CONSTANTINESCU, J. Radioanal. Nucl. Chem., 208 (1996) 461.
5. D. SCHUMANN, S. FISCHER, R. DRESSLER, ST. TAUT, H. NITSCHE, N. TRAUTMANN, M. SCHÄDEL, W. BRÜCHLE, B. SCHAUSTEN, A. F. NOVGORODOV, R. MISIAK, B. EICHLER, H. GÄGGELER, D. JOST, A. TÜRLER, H. BRUCHERTSEIFER, Radiochim. Acta, 72 (1996) 137.
6. D. TRUBERT, F. MONROY GUZMAN, C. LE NAOUR, L. BRILLARD, M. HUSSONNOIS, O. CONSTANTINESCU, Anal. Chim. Acta, 374 (1998) 149.
7. K. E. GREGORICH, R. A. HENDERSON, D. M. LEE, M. J. NURMIA, R. M. CHASTELER, H. L. HALL, D. A. BENNETT, C. M. GANNETT, R. B. CHADWICK, J. D. LEYBA, D. C. HOFFMAN, G. HERRMANN, Radiochim. Acta, 43 (1988) 223.
8. J. V. KRATZ, H. P. ZIMMERMANN, U. W. SCHERER, M. SCHÄDEL, W. BRÜCHLE, K. E. GREGORICH, C. M. GANNETT, H. L. HALL, R. A. HENDERSON, D. M. LEE, J. D. LEYBA, M. J. NURMIA, D. C. HOFFMAN, H. GÄGGELER, D. JOST, U. BALTENSPERGER, YA NAI-QI, A. TÜRLER, CH. LIENERT, Radiochim. Acta, 48 (1989) 121.
9. M. K. GOBER, J. V. KRATZ, H. P. ZIMMERMANN, M. SCHÄDEL, W. BRÜCHLE, E. SCHIMPF, K. E. GREGORICH, A. TÜRLER, N. J. HANNINK, K. R. CZERWINSKI, B. KADKHODAYAN, D. M. LEE, M. J. NURMIA, D. C. HOFFMAN, H. GÄGGELER, D. JOST, J. KOVACS, U. W. SCHERER, A. WEBER, Radiochim. Acta, 57 (1992) 77.
10. M. SCHÄDEL, W. BRÜCHLE, E. SCHIMPF, H. P. ZIMMERMANN, M. K. GOBER, J. V. KRATZ, N. TRAUTMANN, H. GÄGGELER, D. JOST, J. KOVACS, U. W. SCHERER, A. WEBER, K. E. GREGORICH, A. TÜRLER, K. R. CZERWINSKI, N. J. HANNINK, B. KADKHODAYAN, D. M. LEE, M. J. NURMIA, D. C. HOFFMAN, Radiochim. Acta, 57 (1992) 85.
11. H. P. ZIMMERMANN, M. K. GOBER, J. V. KRATZ, M. SCHÄDEL, W. BRÜCHLE, E. SCHIMPF, K. E. GREGORICH, A. TÜRLER, K. R. CZERWINSKI, N. J. HANNINK, B. KADKHODAYAN, D. M. LEE, M. J. NURMIA, D. C. HOFFMAN, H. GÄGGELER, D. JOST, J. KOVACS, U. W. SCHERER, A. WEBER, Radiochim. Acta, 60 (1993) 11.
12. W. PAULUS, J. V. KRATZ, E. STRUB, S. ZAUNER, W. BRÜCHLE, V. PERSHINA, M. SCHÄDEL, B. SCHAUSTEN, J. L. ADAMS, K. E. GREGORICH, D. C. HOFFMAN, M. R. LANE, C. LAUE, D. M. LEE, C. A. MCGRATH, D. K. SHAUGHNESSY, D. A. STRELLIS, E. R. SYLWESTER, J. Alloys Comp., 271–273 (1998) 292.
13. W. PAULUS, J. V. KRATZ, E. STRUB, S. ZAUNER, W. BRÜCHLE, V. PERSHINA, M. SCHÄDEL, B. SCHAUSTEN, J. L. ADAMS, K. E. GREGORICH, D. C. HOFFMAN, M. R. LANE, C. LAUE, D. M. LEE, C. A. MCGRATH, D. K. SHAUGHNESSY, D. A. STRELLIS, E. R. SYLWESTER, Radiochim. Acta, 84 (1999) 69.
14. Y. NAGAME, H. HABA, K. TSUKADA, M. ASAI, A. TOYOSHIMA, S. GOTO, K. AKIYAMA, T. KANEKO, M. SAKAMA, M. HIRATA, T. YAITA, I. NISHINAKA, S. ICHIKAWA, H. NAKAHARA, Nucl. Phys., A734 (2004) 124.

15. YU. TS. OGANESSIAN, V. K. UTYONKOV, S. N. DMITRIEV, YU. V. LOBANOV, M. G. ITKIS, A. N. POLYAKOV, YU. S. TSYGANOV, A. N. MEZENTSEV, A. V. YEREMIN, A. A. VOINOV, E. A. SOKOL, G. G. GULBEKIAN, S. L. BOGOMOLOV, S. ILIEV, V. G. SUBBOTIN, A. M. SUKHOV, G. V. BUKLANOV, S. V. SHISHKIN, V. I. CHEPYGIN, G. K. VOSTOKIN, N. V. AKSENOV, M. HUSSONNOIS, K. SUBOTIC, V. I. ZAGREBAEV, K. J. MOODY, J. B. PATIN, J. F. WILD, M. A. STOYER, N. J. STOYER, D. A. SHAUGHNESSY, J. M. KENNEALLY, P. A. WILK, R. W. LOUGHEED, H. W. GÄGGELER, D. SCHUMANN, H. BRUCHERTSEIFER, R. EICHLER, Phys. Rev., C72 (2005) 034611.
16. D. SCHUMANN, H. BRUCHERTSEIFER, R. EICHLER, B. EICHLER, H. W. GÄGGELER, S. N. DMITRIEV, YU. TS. OGANESSIAN, V. K. UTYONKOV, S. V. SHISHKIN, A. V. YEREMIN, YU. V. LOBANOV, Y. S. TSYGANOV, V. I. CHEPYGIN, E. A. SOKOL, G. K. VOSTOKIN, N. V. AKSENOV, M. HUSSONNOIS, M. G. ITKIS, Radiochim. Acta, 93 (2005) 727.
17. H. HABA, K. TSUKADA, M. ASAI, A. TOYOSHIMA, K. AKIYAMA, I. NISHINAKA, M. HIRATA, T. YAITA, S. ICHIKAWA, Y. NAGAME, K. YASUDA, Y. MIYAMOTO, T. KANEKO, S. GOTO, S. ONO, T. HIRAI, H. KUDO, M. SHIGEKAWA, A. SHINOHARA, Y. OURA, H. NAKAHARA, K. SUEKI, H. KIKUNAGA, N. KINOSHITA, N. TSURUGA, A. YOKOYAMA, M. SAKAMA, S. ENOMOTO, M. SCHÄDEL, W. BRÜCHLE, J. V. KRATZ, J. Am. Chem. Soc., 126 (2004) 5219.
18. A. TOYOSHIMA, H. HABA, K. TSUKADA, M. ASAI, K. AKIYAMA, S. GOTO, Y. ISHII, I. NISHINAKA, T. K. SATO, Y. NAGAME, W. SATO, Y. TANI, H. HASEGAWA, K. MATSUO, D. SAIKA, Y. KITAMOTO, A. SHINOHARA, M. ITO, J. SAITO, H. KUDO, A. YOKOYAMA, M. SAKAMA, K. SUEKI, Y. OURA, H. NAKAHARA, M. SCHÄDEL, W. BRÜCHLE, J. V. KRATZ, Radiochim. Acta, in press.
19. Y. NAGAME, K. TSUKADA, M. ASAI, A. TOYOSHIMA, K. AKIYAMA, Y. ISHII, T. KANEKO-SATO, M. HIRATA, I. NISHINAKA, S. ICHIKAWA, H. HABA, S. ENOMOTO, K. MATSUO, D. SAIKA, Y. KITAMOTO, H. HASEGAWA, Y. TANI, W. SATO, A. SHINOHARA, M. ITO, J. SAITO, S. GOTO, H. KUDO, H. KIKUNAGA, N. KINOSHITA, A. YOKOYAMA, K. SUEKI, Y. OURA, H. NAKAHARA, M. SAKAMA, M. SCHÄDEL, W. BRÜCHLE, J. V. KRATZ, Radiochim. Acta, 93 (2005) 519.
20. Y. KASAMATSU, A. TOYOSHIMA, H. TOUME, K. TSUKADA, H. HABA, Y. NAGAME, J. Nucl. Radiochem. Sci., 8 (2007) 69.
21. M. PLAISANCE, R. GUILLAUMONT, Radiochim. Acta, 12 (1969) 32.
22. K. AKIYAMA et al., to be submitted.
23. O. L. KELLER, A. CHETHAN-STRODE, Inorg. Chem., 5 (1966) 367.
24. M. N. BUKHSH, J. FLEGENHEIMER, F. M. HALL, A. G. MADDOCK, C. F. MIRANDA, J. Inorg. Nucl. Chem., 28 (1966) 421.
25. J. I. KIM, H. LAGALLY, H. J. BORN, Anal. Chim. Acta, 64 (1973) 29.
26. B. F. MYASOEDOV, H. W. KIRBY, I. G. TANANAEV, Protactinium, in: The Chemistry of the Actinide and Transactinide Elements, Vol. 1, L. R. MORSS, N. M. EDELSTEIN, J. FUGER (Eds), 3rd ed., Springer, Dordrecht, The Netherlands, 2006, p. 213.
27. R. CALETKA, V. KRIVAN, J. Radioanal. Nucl. Chem., 142 (1990) 359.

Radiochim. Acta 96, 323–326 (2008) / DOI 10.1524/ract.2008.1498

Development of an electrochemistry apparatus for the heaviest elements

By A. Toyoshima[1,*], Y. Kasamatsu[1], Y. Kitatsuji[2], K. Tsukada[1], H. Haba[3], A. Shinohara[4] and Y. Nagame[1]

[1] Advanced Science Research Center, Japan Atomic Energy Agency, Tokai, Ibaraki 319-1195, Japan
[2] Nuclear Science and Engineering Directorate, Japan Atomic Energy Agency, Tokai, Ibaraki 319-1195, Japan
[3] Nishina Center for Accelerator Based Science, RIKEN, Wako, Saitama 351-0198, Japan
[4] Department of Chemistry, Osaka University, Toyonaka, Osaka 560-0043, Japan

(Received October 12, 2007; accepted in revised form November 21, 2007)

Electrochemistry / Flow electrolytic cell / Chemically modified electrode / Redox reaction

Summary. We developed a new apparatus for the study of electrochemical properties of the heaviest elements. The apparatus is based on a flow electrolytic cell combined with column chromatography. Glassy-carbon fibers modified with Nafion perfluorinated cation-exchange resin are used as a working electrode as well as a cation-exchanger. The elution behavior of ^{139}Ce with the number of 10^{10} atoms in 0.1 M ammonium α-hydroxyisobutyric acid solution from the column electrode was investigated at the applied potentials of 0.2–1.0 V versus the Ag/AgCl reference electrode in 1.0 M LiCl. It was found that $^{139}Ce^{3+}$ is successfully oxidized to $^{139}Ce^{4+}$ even with tracer concentration at around the redox potential determined by cyclic voltammetry for the macro amounts of Ce with 10^{17} atoms (10^{-3} M). The present oxidation reaction and separation of Ce^{4+} was accomplished within a few minutes.

1. Introduction

The heaviest atoms with atomic numbers ≥ 101 must be produced in heavy-ion-induced nuclear reactions. Because of the short half-lives and the low production rates, chemical experiments are carried out on an atom-at-at-time basis. According to the concept of single-atom chemistry by Guillaumont *et al.* [1,2], it is suggested that an equilibrium constant of the atom between two phases is correctly determined in terms of the probability of finding the atoms in one phase or the other. Thus, currently favorable experimental techniques for the chemical study of the heaviest elements are based on partition methods such as ion-exchange chromatography, solvent extraction, and gas chromatography [3,4].

Oxidation-reduction (redox) studies of the heaviest elements are expected to give valuable information on valence electron states such as oxidation states and redox potentials. Ordinary electrochemical approaches such as cyclic voltammetry are, however, not available for the single-atom chemistry of the heaviest elements. Thus, one needs to investigate redox properties of the heaviest elements based on partition behavior of the single atoms between two phases instead of measurement of electric currents arising from a redox reaction.

Radiochemical polarography has been applied to the determination of the amalgamation potentials of element 101 (mendelevium, Md) [5] and element 102 (nobelium, No) [6, 7] where amalgamated metals were extracted into the mercury phase from aqueous solution. The amalgamation technique gives reduction potentials from the most stable oxidation states to amalgamated metallic-states.

Another technique is the column chromatography with simultaneous use of reducing and oxidizing agents, which is based on differences in adsorption abilities between ions with different oxidation states. The existence of the divalent state of Md [8–10] and the trivalent one of No [11, 12] in aqueous solutions has been verified based on the chromatographic behavior comparing with that of some indicative radiotracers. It is, however, difficult to apply this technique to the heavier elements with shorter half-lives because of the time-consuming and complicated procedures.

In the present study, we newly developed an electrochemistry apparatus to identify possible oxidation states of the heaviest elements in aqueous solutions. The apparatus is based on a flow electrolytic cell [13–15] equipped with a chemically modified electrode [16–19] that is quite suitable for rapid and efficient chemical experiments of the heaviest elements. A chemically modified method was applied to separate ions of interest in different oxidation states on the electrode. We studied the oxidation reaction of $Ce^{3+} \rightarrow Ce^{4+} + e^-$ with macro- and tracer-amounts of concentration of Ce in 0.1 M ammonium α-hydroxyisobutyric acid (α-HIB) solution by separating Ce^{3+} and Ce^{4+} in elution procedures. First, cyclic voltammetry of Ce with 10^{17} atoms (10^{-3} M) in 0.1 M α-HIB solution was performed to determine the redox potential of the $Ce^{4+} + e^- \rightleftarrows Ce^{3+}$ reaction under the present condition. Then, the elution behavior of the radiotracer ^{139}Ce with 10^{10} atoms on the chemically modified electrode was investigated at the applied potentials of 0.2–1.0 V. The applicability of the present apparatus to single-atom chemistry is demonstrated.

*Author for correspondence
(E-mail: toyoshima.atsushi@jaea.go.jp).

2. Experimental

2.1 Electrochemistry apparatus

The electrochemistry apparatus developed is based on the flow electrolytic cell [13–15]. A cross sectional view of the apparatus is illustrated in Fig. 1. The working electrode is made of a bundle of glassy-carbon fibers of 11 μm average diameter (GC-20, Tokai Carbon co. ltd.) that is packed in a porous Vycor glass tube (4.8 mm i.d., 7 mm o.d., 30 mm long, Corning co., ltd.) which works as an electrolytic diaphragm. The number of the packed carbon fibers and the total surface area are calculated to be approximately 1.4×10^5 and 1500 cm^2, respectively.

The surface of the carbon fibers was modified with Nafion perfluorinated cation-exchange resin (Nafion dispersion solution DE2020, Wako Chemicals). A bundle of carbon fibers were soaked in 1% Nafion solution diluted with acetone. Then, the solution was evaporated at room temperature. The modified fibers were packed in the Vycor glass tube. The glass tube sealed with o-rings at both sides was installed in the electrolyte pool that was filled with 0.1 M α-HIB. A platinum-mesh counter electrode was placed in the pool to surround the glass tube. The potential on the working electrode was controlled using a potentiostat (Hokuto Denko, HB111) referring to the 1.0 M LiCl-Ag/AgCl electrode placed in the pool.

2.2 Cyclic voltammetry of Ce

Cyclic voltammetry of Ce in 0.1 M α-HIB solution (pH 3.9) was performed at a scan rate of 20 $mV\,s^{-1}$ using the electrochemistry apparatus to determine the redox potential of the $Ce^{4+} + e^- \rightleftarrows Ce^{3+}$ reaction under the present condition. The 10^{-3} M Ce^{3+} solution was prepared from the reagent $Ce(NO_3)_3 \cdot 6H_2O$. A carbon-fiber electrode without modification by Nafion was used in the non-flow mode to measure the current caused by the redox reaction of Ce.

2.3 Production of radiotracers

The nuclide ^{139}Ce ($T_{1/2} = 137.64$ d) was produced in the $^{139}La(p, n)^{139}Ce$ reaction at the RIKEN K70 AVF Cyclotron, while those of ^{88}Zr ($T_{1/2} = 83.4$ d), ^{175}Hf ($T_{1/2} = 70.2$ d), and ^{85}Sr ($T_{1/2} = 64.84$ d) were produced in the $^{89}Y(p, 2n)$, $^{175}Lu(p, n)$, and $^{85}Rb(p, n)$ reactions, respectively, at the JAEA tandem accelerator. These radiotracers were separated from the relevant target materials by ion-exchange methods, and ^{88}Y ($T_{1/2} = 106.65$ d) generated from the EC-decay of ^{88}Zr was also prepared. They were stored in 0.1 M α-HIB solution. The radiotracers except ^{139}Ce were used as the references of the typical oxidation states in α-HIB solution: Zr^{4+}, Hf^{4+}, Y^{3+}, and Sr^{2+}.

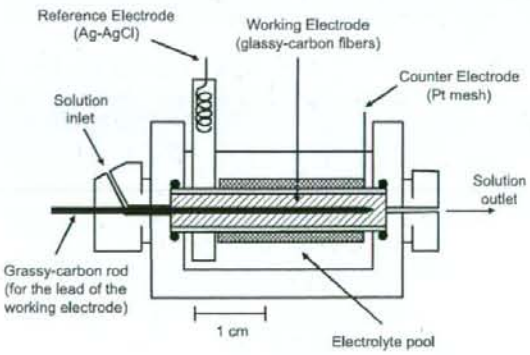

Fig. 1. Schematic view of the electrochemistry apparatus.

2.4 Cation-exchange experiments of Ce^{3+} and Ce^{4+}

Prior to the electrochemical study, it is indispensable to examine the different elution behavior of Ce^{3+} and Ce^{4+} under the present conditions. The elution behavior of Ce^{3+} and Ce^{4+} of 10^{-4} M in 0.1 M α-HIB solution from a strongly acidic cation-exchange column was studied.

The samples of Ce^{3+} and Ce^{4+} were prepared from the $Ce(NO_3)_3 \cdot 6H_2O$ and $(NH_4)_2[Ce(NO_3)_6]$ reagents, respectively, and were separately stored in the 0.1 M α-HIB solution (pH 4.0) together with the radiotracers of ^{139}Ce, ^{88}Zr, ^{175}Hf, ^{88}Y, and ^{85}Sr. It is noted that the samples with Ce^{4+} were subjected to the cation-exchange experiments after preparation as soon as possible because Ce^{4+} is gradually reduced to Ce^{3+} in the 0.1 M α-HIB solution within a few tens of minutes.

200 μL of the 0.1 M α-HIB including 10^{-4} M Ce and the radiotracers was fed onto the cation-exchange column (MCI GEL CK08Y, 1.6 mm i.d. ×7.0 mm long) at a flow rate of 1 $mL\,min^{-1}$. Then, 2400 μL of the 0.1 M α-HIB solution was subsequently fed onto the column. The effluents were fractionated into 8 aliquots in plastic tubes. The remaining elements on the column were then eluted with 400 μL of 6.0 M HNO_3. The effluent was also collected in a plastic tube. All effluent samples were assayed for γ-ray activity using a Ge detector.

2.5 Electrochemical oxidation of ^{139}Ce

The Nafion perfluorinated ion-exchange resin on the working electrode was preconditioned by passing 0.1 M α-HIB solution (pH 3.9) through the column. Then, 200 μL of the 0.1 M α-HIB solution (pH 3.9) including radiotracers of ^{139}Ce, ^{88}Zr, ^{175}Hf, ^{88}Y, and ^{85}Sr was fed onto the column electrode followed by feeding 1800 μL of α-HIB solution (pH 3.9). The potential applied to the electrode was adjusted to 0.2, 0.7, 0.75, 0.8, and 1.0 V using the potentiostat. The effluent from the outlet was fractionated into 13 aliquots in plastic tubes at each potential. The remaining radiotracers on the electrode were eluted with 1000 μL of 3.0 M HCl at 0.2 V, and the effluent was collected in another plastic tube. These chromatographic separation procedures were completed within a few minutes. All effluent samples were assayed for γ-ray activity using a Ge detector. The number of ^{139}Ce atoms used for each experiment was 10^{10}. Chemical yields of these radiotracers were evaluated to be about 90%.

3. Results and discussion

Fig. 2 shows the voltamogram of 10^{-3} M Ce in 0.1 M α-HIB solution. The abscissa represents the applied potential and

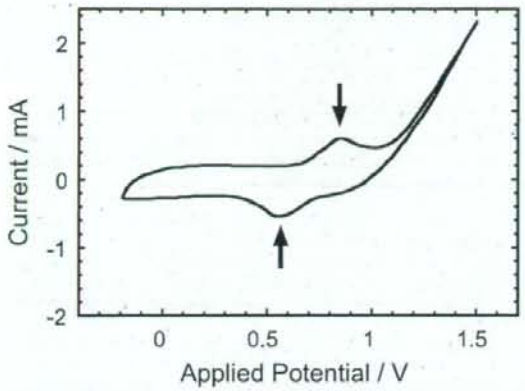

Fig. 2. Voltamogram of 10^{-3} M cerium in 0.1 M α-hydroxyisobutyric solution (pH 3.9) with the 1.0 M LiCl–Ag/AgCl reference electrode. The abscissa represents the applied potential and the ordinate the measured current. The arrows indicate the current peaks observed.

the ordinate shows the observed current. The positive current caused by the oxidation reaction of $Ce^{3+} \rightarrow Ce^{4+} + e^-$ is at around 0.85 V, while the negative current through the inverse reaction is observed around 0.55 V. Thus, the formal redox potential of the $Ce^{4+} + e^- \rightleftarrows Ce^{3+}$ reaction in the present solution is measured to be 0.7 V that is equivalent to 0.92 V referred to the standard hydrogen electrode (SHE). This formal potential is, however, much lower than the potential of 1.7 V in 1 M $HClO_4$ solution [19] versus the SHE reference, which is due to complex formation of Ce with the α-HIB ligands which lowers the redox potential of the reaction.

Fig. 3(a) and 3(b) show the elution curves of 10^{-4} M Ce^{3+} and 10^{-4} M Ce^{4+}, respectively, on the cation-exchanger.

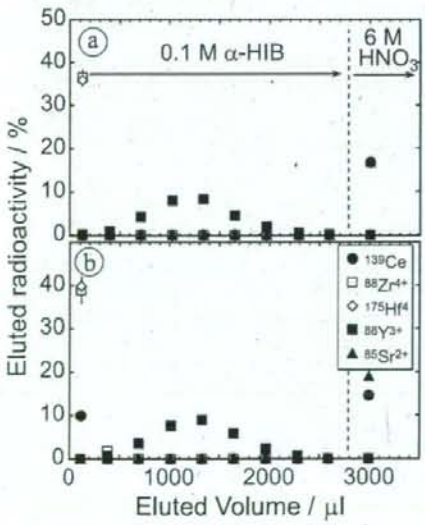

Fig. 3. Elution curves of (a) 10^{-3} M Ce^{3+} and (b) 10^{-3} M Ce^{4+} together with the carrier-free ^{85}Sr, ^{88}Y, ^{88}Zr, and ^{175}Hf radiotracers in 0.1 M α-hydroxyisobutyric solution (pH 4.0) on the cation-exchange column (CK08Y resin).

Eluted radioactivities per 100 µL of the effluent for ^{139}Ce, ^{88}Zr, ^{175}Hf, ^{88}Y, and ^{85}Sr are depicted. It is found that Ce^{3+} is strongly adsorbed on the resin in the α-HIB solution and is stripped from the column with the 6 M HNO_3, while Ce^{4+} is sooner eluted in the α-HIB solution although a part of Ce^{4+} was already reduced to Ce^{3+}. The stronger adsorbability of Ce^{3+} compared with that of Y^{3+} on the cation-exchange resin is qualitatively consistent with the elution behavior reported in Ref. [21]. The elution behavior of Ce^{4+} is similar to that of Zr^{4+} and Hf^{4+}.

Fig. 4(a)–(e) show the elution curves of ^{139}Ce, ^{88}Zr, ^{175}Hf, ^{88}Y, and ^{85}Sr from the modified electrode at the applied potentials of 0.2, 0.7, 0.75, 0.8, and 1.0 V, respectively. The ordinate shows the eluted radioactivities per 100 µL of the effluent. The results of the fit according to the Glückauf

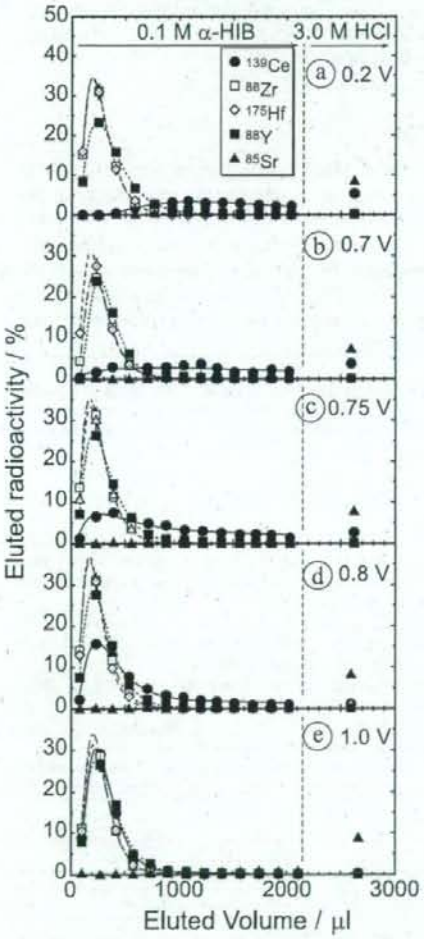

Fig. 4. Elution curves of the carrier free ^{139}Ce radiotracer at the applied potentials of (a) 0.2 V, (b) 0.7 V, (c) 0.75 V, (d) 0.8 V, and (e) 1.0 V relative to the 1.0 M LiCl–Ag/AgCl electrode. Eluted radioactivities of ^{85}Sr, ^{88}Y, ^{139}Ce, ^{88}Zr and ^{175}Hf are depicted by open triangles, open circles, closed circles, open squares, and open diamonds, respectively. Lines demonstrate fits according to the Glückauf model of chromatography.

model [22] of chromatography were shown as solid lines, dashed and dotted lines, broken lines, and dotted lines for ^{139}Ce, ^{88}Zr,^{175}Hf, and ^{88}Y, respectively. At the lowest potential of 0.2 V in Fig. 4(a), the elution order of the radiotracers, $Zr^{4+} \approx Hf^{4+} > Y^{3+} > Ce^{3+} > Sr^{2+}$, agrees with that on the CK08Y column shown in Fig. 3(a). This elution behavior shows that the cation-exchange separation on the Nafion electrode is successfully performed although the separation ability on the Nafion electrode is worse. It is noted that ^{139}Ce is bound in the most stable trivalent state at this potential. On the other hand, at the highest potential of 1.0 V in Fig. 4(e), the elution of ^{139}Ce agrees well with that of Zr^{4+} and Hf^{4+}, and that of 10^{-4} M Ce^{4+} on the CK08Y resin in Fig. 3(b). This clearly demonstrates that $^{139}Ce^{3+}$ is electrochemically oxidized to Ce^{4+} on the modified electrode. Comparing the elution behavior of ^{139}Ce in Fig. 4(a) to 4(e), the fractions of $^{139}Ce^{4+}$ increase with increasing the applied potential while no variation was observed in the elution of the other elements, which reveal that $^{139}Ce^{3+}$ is oxidized to $^{139}Ce^{4+}$ around the redox potential of 0.7 V.

4. Conclusion

Oxidation of Ce in tracer concentration was successively conducted using the newly developed electrochemical apparatus. The redox potential of ^{139}Ce with the 10^{10} atoms (10^{-11} M) evaluated from its elution behavior was consistent with that determined in the current measurement with the macro amount of Ce (10^{-3} M). The rapid procedure taking a few minutes is well suitable for the electrochemical study of the heaviest elements.

Acknowledgment. We are indebted to Dr. Z. Yoshida for his fruitful advice and suggestions. We thank the crew of the JAEA tandem accelerator facility and of the RIKEN K70 AVF Cyclotron for their beam operations.

References

1. Guillaumont, R., Adloff, J. P., Peneloux, A.: Kinetic and thermodynamic aspects of tracer-scale and single atom chemistry. Radiochim. Acta **46**, 169 (1989).
2. Guillaumont, R., Adloff, J. P., Peneloux, A., Delamoye, P.: Subtracer scale behaviour of radionuclides. Application to actinide chemistry. Radiochim. Acta **54**, 1 (1991).
3. Schädel, M.: Chemistry of superheavy elements. Angew. Chem. Int. Edit. **45**, 368 (2006).
4. Schädel, M. (ed.): *The Chemistry of Superheavy Elements*. Kluwer Academic Publishers, Dordrecht (2003).
5. David, F., Samhoun, K., Hulet, E. K., Baisden, P. A., Dougan, R., Landrum, J. H., Lougheed, R. W., Wild, J. F., O'Kelley, G. D.: Radiopolarography of mendelevium in aqueous solutions. J. Inorg. Nucl. Chem. **43**, 2941 (1981).
6. Meyer, R. E., McDowell, W. J., Dittner, P. F., Silva, R. J., Tarrant, J. R.: Determination of the half-wave potential of nobelium. J. Inorg. Nucl. Chem. **38**, 1171 (1976).
7. David, F., Samhoun, K., Lougheed, R. W., Dougan, R. J., Wild, J. F., Landrum, J. H., Dougan, A. D., Hulet, E. K.: Electrochemical reduction and related thermodynamic properties of nobelium. Radiochim. Acta **51**, 65 (1990).
8. Hulet, E. K., Lougheed, R. W., Brady, J. D., Stone, R. E, Coops, M. S.: Mendelevium: divalency and other chemical properties. Science **158**, 486 (1967).
9. Guseva, L. I., Tikhomirova, G. S., Buklanov, G. V., Phar, Z. Z., Levedev, I. A., Katargin, N. V., Myasoedov, B. F.: Isolation and ion exchanging behavior of mendelevium(II). J. Radioanal. Nucl. Chem. Lett. **117**, 205 (1987).
10. Scherer, U. W., Kratz, J. V., Schädel, M., Brüchle, W., Gregorich, K. E., Henderson, R. A., Lee, D., Nurmia, M., Hoffman, D. C.: Lawrencium chemistry: No evidence for oxidation states lower than 3+ in aqueous solution. Inorg. Chim. Acta **146**, 249 (1988).
11. Maly, J., Sikkeland, T., Silva, R., Ghiorso, A.: Nobelium: Tracer chemistry of the divalent and trivalent ions. Science **160**, 1114 (1968).
12. Silva, R. J., Sikkeland, T., Nurmia, M., Ghiorso, A., Hulet, E. K.: Determination of the No(II)–No(III) potential from tracer experiments. J. Inorg. Nucl. Chem. **31**, 3405 (1969).
13. Kihara, S., Yoshida, Z., Muto, H., Aoyagi, H., Baba, Y., Hashitani, H.: Determination of oxidation states of uranium in uranium dioxide pellets by two-step flow-coulometry. Anal. Chem. **52**, 1601 (1980).
14. Takeishi, H., Muto, H., Aoyagi, H., Adachi, T., Izawa, K., Yoshida, Z., Kawamura, H.: Determination of oxygen/uranium ratio in irradiated uranium dioxide based on dissolution with strong phosphoric acid. Anal. Chem. **58**, 458 (1986).
15. Aoyagi, H., Yoshida, Z., Kihara, S.: Plutonium and uranium ion determination and differentiation on twin electrode flow coulometry. Anal. Chem. **59**, 400 (1987).
16. Martin, C. R., Freiser, H.: Ion-selective electrodes based on an ionic polymer. Anal. Chem. **53**, 902 (1981).
17. Izutsu, K., Nakamura, T., Ando, T.: Voltammetric determination of uranium in sea water after preconcentration on the trioctylphosphine oxide-coated glassy carbon electrode. Anal. Chim. Acta, **152**, 285 (1983).
18. Espensheid, M. W., Ghatak-Roy, A. R., Moore III, R. B., Penner, R. M., Szentirmay, M. N., Martin, C. R.: Sensors from polymer modified electrodes. J. Chem. Soc. Faraday Trans. 1 **82**, 1051 (1986).
19. Huiliang, H., Jagner, D., Renman, L.: Carbon fibre Electrodes in flow potentiometric stripping analysis. Anal. Chim. Acta **207**, 17 (1988).
20. Morss, L. R.: *Standard Potentials in Aqueous Solution*. (Bard, A. J., Parsons, R., Jordan, J., eds.) International Union of Pure and Applied Chemistry, New York (1985), p. 587.
21. Nash, K. L.: *Handbook on the Physics and Chemistry of Rare Earths, Vol. 18 Lanthanides/Actinides: Chemistry*. (Gschneidner Jr., K. A., Eyring, L., Choppin, G. R., Lander, G. H., eds.) Elsevier Science, Amsterdam (1994), p. 197.
22. Glückauf, E.: Theory of chromatography. Part 9. The "theoretical plate" concept in column separations. Trans. Faraday Soc. **51**, 34 (1955).

Journal of Nuclear and Radiochemical Sciences, Vol. 9, No.1, pp. 27-31, 2008

Performance of the Gas-jet Transport System Coupled to the RIKEN Gas-filled Recoil Ion Separator GARIS for the $^{238}U(^{22}Ne, 5n)^{255}No$ Reaction

H. Haba,[a,*] H. Kikunaga,[a,b] D. Kaji,[a] T. Akiyama,[a,c] K. Morimoto,[a] K. Morita,[a] T. Nanri,[d] K. Ooe,[b] N. Sato,[a,e] A. Shinohara,[b] D. Suzuki,[d] T. Takabe,[b] I. Yamazaki,[d] A. Yokoyama,[d] and A. Yoneda[a]

[a]*Nishina Center for Accelerator Based Science, RIKEN, Wako, Saitama 351-0198, Japan*
[b]*Graduate School of Science, Osaka University, Toyonaka, Osaka 560-0043, Japan*
[c]*Department of Physics, Saitama University, Sakura, Saitama 338-8570, Japan*
[d]*Faculty of Science, Kanazawa University, Kanazawa, Ishikawa 920-1192, Japan*
[e]*Department of Physics, Tohoku University, Aoba, Sendai 980-8578, Japan*

Received: May 1, 2008; In Final Form: June 27, 2008

The performance of the gas-jet transport system coupled to the RIKEN gas-filled recoil ion separator GARIS was investigated using ^{255}No produced in the $^{238}U(^{22}Ne, 5n)^{255}No$ reaction. Alpha particles of ^{255}No separated with GARIS and transported by the gas-jet system were measured with a rotating wheel apparatus for α spectrometry under low background condition. The high gas-jet efficiencies of about 75% were independent of the recoil ranges of ^{255}No in the gas-jet chamber. The present results suggest that the GARIS/gas-jet system is a promising tool for the next-generation superheavy element chemistry: (i) the background radioactivities of unwanted reaction products are strongly suppressed, (ii) the intense beam is absent in the gas-jet chamber and hence the high gas-jet efficiency is achieved, and (iii) the beam-free condition also allows for investigations of new chemical systems

1. Introduction

Chemical studies of superheavy elements (SHEs) with atomic numbers $Z \geq 104$ have become one of the most exciting and challenging research subjects in nuclear and radiochemistry.[1,2] The extremely low production yields and short half-lives of SHEs force us to conduct rapid and efficient on-line chemical experiments with "single atoms". Using a gas-jet transport technique, the experimental studies on the chemical properties of SHEs have been performed for elements 104 (Rf) to 108 (Hs) and recently element 112.[1-3] At the same time, many of these successful experiments have clearly demonstrated the limitations of the applied techniques. Large amounts of background radioactivities from unwanted reaction products become unavoidable with increasing Z of SHEs of interest. High-intensity beams from advanced heavy-ion accelerators also give rise to a problem in that the plasma formed by the beam in the target chamber significantly reduces the gas-jet transport efficiency. To overcome these limitations, the concept of physical preseparation of SHE atoms has been proposed.[1,4] With this method, background radioactivities originating from unwanted reaction products are largely removed. The high and stable gas-jet efficiencies are achieved owing to the condition free from plasma. Furthermore, this beam-free condition allows us investigations of new chemical systems that were not accessible before.[4] The pioneering experiments with the recoil transfer chamber (RTC) coupled to the Berkeley Gas-filled Separator (BGS) were very successful.[5,6] The isotope of ^{257}Rf physically separated from the large amount of β-decaying products was identified with a liquid scintillator after a liquid-liquid solvent extraction. Thereafter, the BGS/RTC system was used in the model experiments of Rf[7-9] and Hs.[10] At Gesellschaft für Schwerionenforschung (GSI), a new gas-filled separator, the TransActinide Separator and Chemistry Apparatus (TASCA), is under commissioning as a preseparator for chemical studies.[4,11]

In the RIKEN Linear Accelerator (RILAC) facility, a gas-jet transport system was installed at the focal plane of the RIKEN gas-filled recoil ion separator GARIS to start the SHE chemistry.[12] The performance of the system was first appraised using ^{206}Fr and ^{245}Fm produced in the $^{169}Tm(^{40}Ar, 3n)^{206}Fr$ and $^{208}Pb(^{40}Ar, 3n)^{245}Fm$ reactions, respectively.[12] Alpha particles of ^{206}Fr and ^{245}Fm separated with GARIS and transported by the gas-jet system were measured with a rotating wheel apparatus for α spectrometry under low background condition. The high gas-jet efficiencies of over 80% were found to be independent of the beam intensity up to 2 particle μA (pμA).

In order to produce SHE nuclides with long half-lives for chemical experiments, further asymmetric fusion reactions based on actinide targets such as ^{238}U, ^{244}Pu, and ^{248}Cm should be considered (hot fusion reactions). However, very small recoil velocities of evaporation residues (ERs) produced by such asymmetric reactions cause serious problems in the operation of a gas-jet system coupled to a gas-filled separator. The transport efficiency of the gas-filled separator drastically decreases with decreasing recoil velocity due to the multiple small-angle scattering in the filling gas. A vacuum window foil, which separates the gas-jet chamber from the gas-filled separator, should be thin enough (≈1 μm as Mylar) to allow ERs to pass though and has to withstand a pressure difference of about 100 kPa. In this work, the performance of the GARIS/gas-jet system for the hot fusion reactions was investigated for the first time using ^{255}No produced in the $^{238}U(^{22}Ne, 5n)^{255}No$ reaction. The ^{255}No atoms preseparated with GARIS were successfully extracted by the gas-jet system to a distant site where the rotating wheel apparatus for α spectrometry was equipped. The setting parameters such as the magnetic field of the separator and the gas-jet conditions were optimized to obtain the highest yield of ^{255}No.

*Corresponding author: haba@riken.jp

Published on Web 06/30/2008

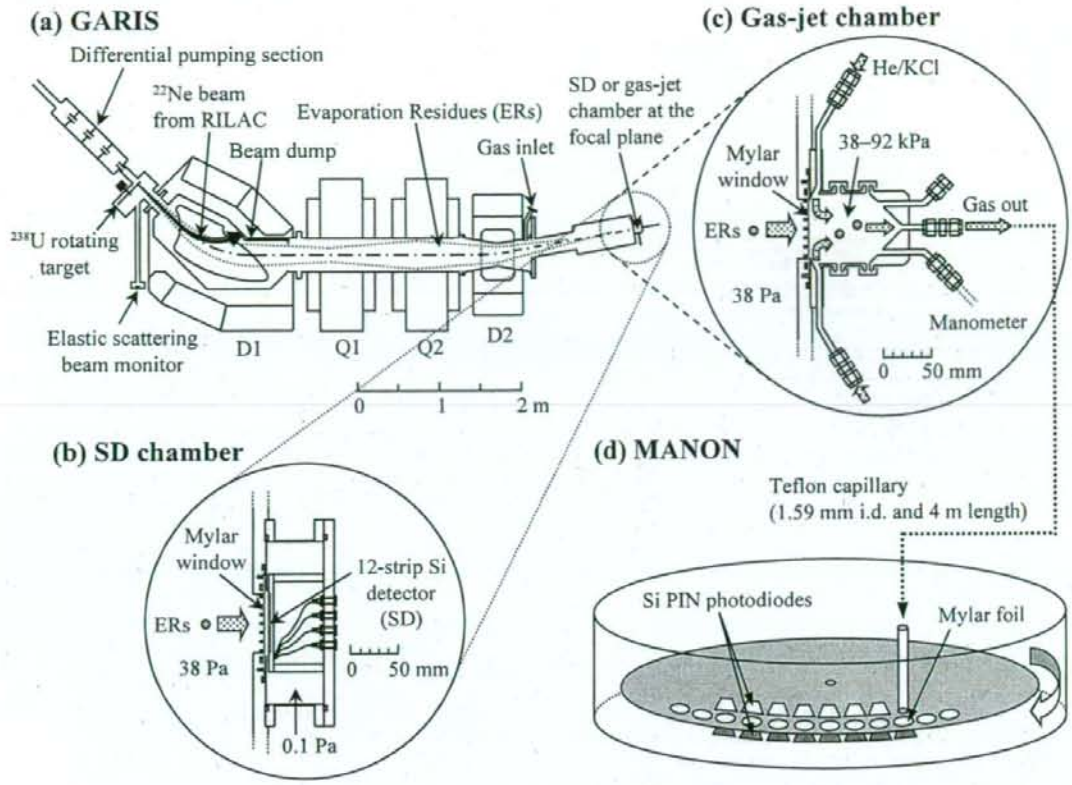

Figure 1. A schematic of the experimental setup: (a) RIKEN gas-filled recoil ion separator GARIS; (b) 12-strip Si detector (SD) chamber; (c) Gas-jet chamber; (d) Rotating wheel apparatus MANON for α spectrometry.

2. Experimental

A schematic of the experimental setup is shown in Figure 1. The $^{22}Ne^{7+}$ ion beam was extracted from RILAC. A $^{238}U_3O_8$ target of 370 μg cm^{-2} thickness was prepared by electrodeposition in 2-propanol onto a 1.27 mg cm^{-2} titanium backing foil. The details of the target preparation are reported elsewhere.[13] Sixteen targets were mounted on a rotating wheel of 30 cm in diameter. The wheel was rotated during the irradiation at 3000 rpm. The beam energy was 113.8 MeV at the middle of the target. At this incident energy, the excitation function for the $^{238}U(^{22}Ne, 5n)^{255}No$ reaction exhibits the maximum cross section of 90 nb.[14] The beam intensity was monitored by measuring elastically scattered projectiles with a Si PIN photodiode (Hamamatsu S1223) mounted at 45° with respect to the beam axis. The typical beam intensity was 4 pμA. GARIS was filled with helium at a pressure of 37 Pa. The other details of GARIS are given elsewhere.[15]

As shown in Figures 1a and 1b, the evaporation residues of interest were separated in-flight from beam particles and transfer reaction products with GARIS, and were implanted into a 12-strip Si detector (SD) of 60 × 60 mm^2 (Hamamatsu 12CH PSD) through a Mylar window foil which was supported with a circular-hole (4.0 mm diameter) grid with 71.6% transparency and of 60 mm diameter. The thickness of the Mylar foil was determined to be 1.1±0.1 μm based on the energy loss of 5.486-MeV α particles from ^{241}Am and on the stopping powers calculated with the SRIM code.[16] The cycle of the beam-on (300 s) and beam-off (600 s) measurements was performed, because no α peaks of ^{255}No were observed in the beam-on spectrum due to large amounts of background events. The α-particle energy resolutions of the 12 SDs were 20–60 keV FWHM. All events were registered in an event-by-event mode using the VME LIST/PHA module (Iwatsu A3100). The magnetic rigidities of 1.73, 1.82, 1.93, and 2.04 T m were examined to optimize the transport efficiency of GARIS for ^{255}No.

In the gas-jet transport experiments, the reaction products separated with GARIS were guided into the stainless-steel gas-jet chamber of 60 mm depth as shown in Figure 1c. The magnetic rigidity was set at 1.93 T m. The ^{255}No atoms were stopped in the helium gas, attached to aerosol particles generated by sublimation of the KCl powder, and were continuously transported through a Teflon capillary (1.59 mm i.d., 4 m length) to the rotating wheel apparatus MANON for α spectrometry (Figure 1d) which was the compact one of the Measurement system for the Alpha-particle and spontaneous fissioN events ON-line developed at Japan Atomic Energy Agency (JAEA).[17] The temperature of the KCl aerosol generator was fixed to 620 °C based on the previous $^{169}Tm(^{40}Ar, 3n)^{206}Fr$ experiment.[12] The flow rates of the helium gas were varied at 1.0, 2.0, 3.0, 4.0, and 5.0 L min^{-1}, which resulted in the inner pressures of the gas-jet chamber of 38, 54, 69, 81, and 92 kPa, respectively. In MANON, the aerosol particles were deposited on 200-position Mylar foils of 0.68 μm thickness placed at the periphery of a stainless steel wheel of 420 mm diameter. The wheel was stepped at 90-s interval to position the foils between seven pairs of Si PIN photodiodes (Hamamatsu S3204-09). Each detector had an active area of 18 × 18 mm^2 and a 38% counting efficiency for α particles. The α-particle energy resolution was 60 keV FWHM for the detectors which look at the sample from the collection side (top detectors).

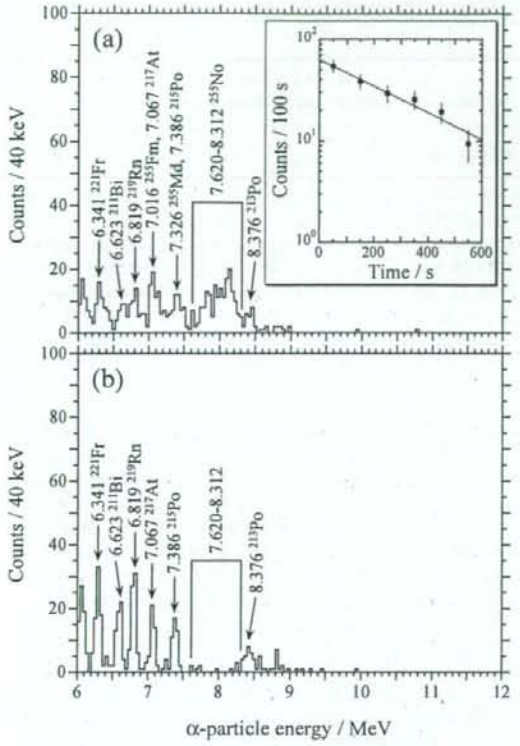

Figure 2. (a) α-Particle spectra measured in the 12-strip Si detector (SD) under the beam-off condition for 36000 s. The ^{22}Ne beam dose of 4.3×10^{17} was accumulated during the cycles of the beam-on (300 s) and beam-off (600 s) measurements. The magnetic rigidity of GARIS was set at 1.93 T m. The inset shows a decay curve of the 7.620–8.312-MeV α peaks of ^{255}No. (b) Background α-particle spectrum measured with SD for 82000 s before the beam experiment.

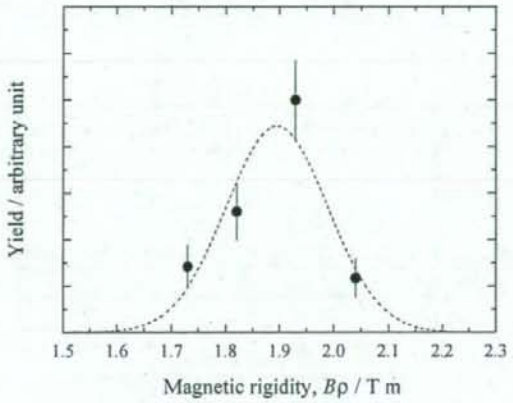

Figure 3. Yield variation of ^{255}No produced in the ^{238}U(^{22}Ne, 5n)^{255}No reaction as a function of the magnetic rigidity of GARIS. The dashed curve represents the result of the least-squares fitting with the Gaussian curve with a maximum yield at $B\rho = 1.89\pm0.02$ T m and a resolution of $\Delta B\rho/B\rho = 12\pm2\%$.

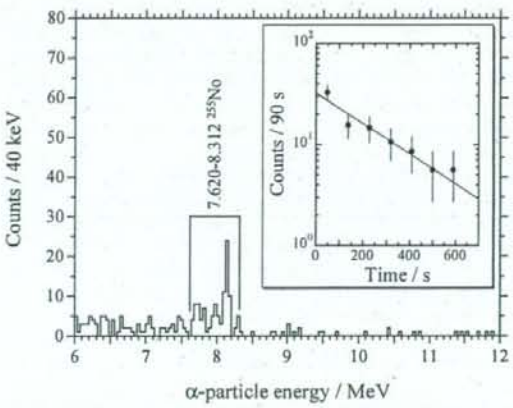

Figure 4. Sum of α-particle spectra measured in the seven top detectors of the rotating wheel apparatus MANON for 630 s after the 90-s aerosol collection. The 90-s aerosol collection was repeated 207 times. The beam dose of 2.8×10^{17} was accumulated. The helium flow rate was 1.0 L min^{-1} and the inner pressure of the gas-jet chamber was 38 kPa.

3. Results and Discussion

As mentioned in the previous section, no α peaks were identified in the α spectrum measured with SD under the beam-on condition (the total count rate of all strips of SD at > 1 MeV is about 2 k counts per second for the 1-pμA beam intensity). Figure 2a shows a sum of α-particle spectra measured in all the strips of SD for 36000 s under the beam-off condition. The beam dose of 4.29×10^{17} was accumulated during the cycles of the beam-on (300 s) and beam-off (600 s) measurements. The magnetic rigidity of GARIS was 1.93 T m. As indicated in Figure 2a, α peaks of ^{255}No were identified in the energy region of interest (E_α = 7.620–8.312 MeV),[18] though many other α peaks are seen in the spectrum. Compared in Figure 2b is a background spectrum measured with SD for 82000 s before the beam experiment. Since SD was contaminated with long-lived ^{225}Ac ($T_{1/2}$ = 10.0 d) and ^{227}Th ($T_{1/2}$ = 18.72 d) which were implanted into SD as transfer reaction products from ^{232}Th in the previous experiment, α lines of their daughter nuclides of ^{221}Fr, ^{211}Bi, ^{219}Rn, ^{217}At, ^{215}Po, and ^{213}Po are clearly identified. Thus, the α peaks in Figure 2a except those for ^{255}No are unambiguously assigned as the background components, though small contributions of the daughter nuclides of ^{255}No, ^{255}Md ($T_{1/2}$ = 27 min, E_α = 7.326 MeV) and ^{255}Fm ($T_{1/2}$ = 20.07 h, E_α = 7.016 MeV), are seen in the spectrum. The decay curve of the 7.620–8.312 MeV α peaks of ^{255}No is shown in the inset of Figure 2a. The half-life of ^{255}No was determined to be 3.8±0.7 min, which is in agreement with the literature value of 3.1±0.2 min.[18] The decay curve also suggests that the contribution of 8.093-MeV α peak of ^{254}No ($T_{1/2}$ = 55 s), which is producible in the ^{238}U(^{22}Ne, 6n)^{254}No reaction, is negligible within the error limit.

In Figure 3, relative yields of ^{255}No are shown as a function of the magnetic rigidity ($B\rho$) of the separator. As shown by a dashed curve in Figure 3, a least-squares fitting with the Gaussian curve gives a maximum yield at $B\rho = 1.89\pm0.02$ T m, where the transport efficiency of GARIS was evaluated to be about 5% for the focal plane of 60 mm diameter, assuming the cross section of the ^{238}U(^{22}Ne, 5n)^{255}No reaction to be 90 nb.[14] The resolution of $\Delta B\rho/B\rho = 12\pm2\%$ suggests that the transport efficiency of GARIS would be increased by a factor of about 2 using the larger focal plane window of 100 mm diameter.

Figure 4 shows the sum of α-particle spectra measured in the seven top detectors of MANON. In this measurement, the beam dose of 2.81×10^{17} was accumulated. The 7.620–8.312-MeV α peaks of ^{255}No are clearly seen in the spectrum, indicating that the gas-jet transport of ^{255}No to MANON was successfully conducted after the physical separation with

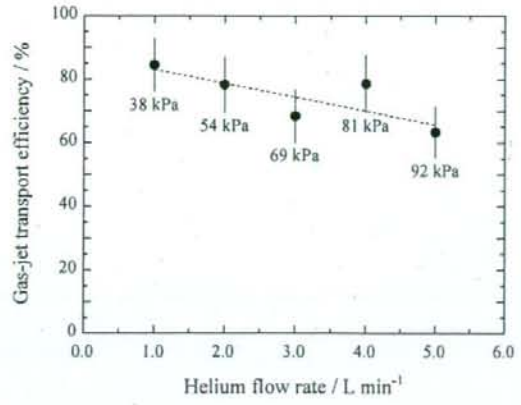

Figure 5. Variation of the gas-jet transport efficiency of ^{255}No as a function of the helium flow rate. The inner pressures of the gas-jet chamber are indicated for each data point.

GARIS. Background radioactivities such as ^{213}Po (8.376-MeV α) and ^{212m}Po (11.650-MeV α), which are largely produced in the transfer reactions on the lead impurity in the target,[19] are fully removed by the present system. The decay curve for the 7.620–8.312-MeV component is shown in the inset of Figure 4a. The half-life was determined to be 3.4±0.8 min. Since MANON was placed in the target room in this experiment, some background events caused by large amounts of neutrons during the irradiation are seen in the spectrum. Recently, we have constructed a chemistry laboratory, which is isolated with a 50-cm concrete shield from the target room, just behind the focal plane of GARIS. In the future, this kind of experiment will be conducted under improved background conditions.

In the conventional gas-jet system in that the beam passes in the target chamber, the gas-jet efficiency decreases due to the increasing plasma induced by the beam. As an example, we measured the gas-jet efficiencies of ^{173}W produced in the ^{nat}Gd(^{22}Ne, *x*n) reaction without the beam separation by GARIS.[14] It was found that the gas-jet efficiency of ^{173}W drastically decreases from 40% at 6.6 pnA to 25% at 0.5 pμA. In Figure 5, the gas-jet transport efficiencies of ^{255}No are shown as a function of the helium flow rate. In this work, the high gas-jet efficiencies of about 75% were achieved even at > 1 pμA owing to the plasma-free condition. It is also found in Figure 5 that the gas-jet efficiencies are independent of the helium flow rate, i.e., the inner pressure of the gas-jet chamber, though a slight decreasing trend is seen. The recoil ranges of ^{255}No in helium at 38–90 kPa are calculated to be 16.0–6.6 mm, respectively, using the LISE++ code.[20] These recoil ranges are short enough as compared with the depth of the gas-jet chamber (60 mm). In our previous study,[12] the high gas-jet efficiencies of over 80% were obtained both for ^{206}Fr and ^{245}Fm. The recoil ranges of ^{206}Fr and ^{245}Fm in helium at 90 kPa were 30 and 18 mm, respectively. In the conventional gas-jet system, where a beam dump is placed in the bottom of the chamber, the gas is swept out through the capillary outlet to the vertical direction of the beam axis. Therefore, the position of the capillary outlet in the chamber should be exactly adjusted to the recoil ranges of the product nuclei to obtain their highest gas-jet yields. In the present system, the beam is separated with GARIS and hence we can put the capillary outlet in the bottom of the chamber (see Figure 1c). Thus, the gas is fed into the chamber through the four inlets directed to the surface of the Mylar window and is swept out thoroughly from the bottom of the chamber. This helium flow path in the gas-jet chamber would be advantageous to the range-independent gas-jet efficiencies. It is finally pointed out that the highest efficiency of ^{255}No is achieved at the lowest chamber pressure of 38 kPa. This enables us to safely handle the thinner Mylar windows of < 1 μm thickness that should be required for SHE nuclides such as ^{261}Rf and ^{262}Db produced in the ^{248}Cm(^{18}O, 5n)^{261}Rf and ^{248}Cm(^{19}F, 5n)^{262}Db reactions, respectively.

4. Summary

We have successfully produced ^{255}No in the hot fusion reaction of ^{238}U(^{22}Ne, 5n)^{255}No using the gas-jet transport system coupled to GARIS. The α particles of ^{255}No separated with GARIS and transported by the gas-jet were clearly observed with a rotating wheel apparatus for α spectrometry. The high gas-jet efficiencies of about 75% were obtained at the beam intensities of over 1 pμA, and they were independent of the recoil ranges of ^{255}No in the gas-jet chamber. These results suggest that the GARIS/gas-jet system is promising to explore new frontiers in SHE chemistry: (i) the background radioactivities originating from unwanted reaction products are strongly suppressed, (ii) the intense primary heavy-ion beam is absent in the gas-jet chamber and hence the high gas-jet efficiency is achieved, and (iii) the beam-free condition also makes it possible to investigate new chemical systems that were not accessible before. In the next phase, we plan to investigate the production of SHE nuclides with long half-lives for chemical experiments such as ^{261}Rf, ^{262}Db, ^{265}Sg, and ^{269}Hs based on the ^{248}Cm target.

Acknowledgement. The authors express their gratitude to the crew of the RIKEN Linear Accelerator for their invaluable assistance in the course of these experiments. This research was partially supported by the Ministry of Education, Science, Sports and Culture, Grant-in-Aid for Young Scientists (B), 16750055, 2004–2006 and (B), 17740179, 2005–2006.

References

(1) M. Schädel, Ed. *The Chemistry of Superheavy Elements*, Kluwer Academic Publishers, Dordrecht, (2003).
(2) M. Schädel, Angew. Chem. Int. Ed. **45**, 368 (2006).
(3) R. Eichler, N. V. Aksenov, A. V. Belozerov, G. A. Bozhikov, V. I. Chepigin, S. N. Dmitriev, R. Dressler, H. W. Gäggeler, V. A. Gorshkov, F. Haenssler, M. G. Itkis, A. Laube, V. Ya. Lebedev, O. N. Malyshev, Yu. Ts. Oganessian, O. V. Petrushkin, D. Piguet, P. Rasmussen, S. V. Shishkin, A. V. Shutov, A. I. Svirikhin, E. E. Tereshatov, G. K. Vostokin, M. Wegrzecki, and A. V. Yeremin, Nature **447**, 72 (2007).
(4) Ch. E. Düllmann, Eur. Phys. J. D **45**, 75 (2007).
(5) J. P. Omtvedt, J. Alstad, H. Breivik, J. E. Dyve, K. Eberhardt, C. M. Folden III, T. Ginter, K. E. Gregorich, E. A. Hult, M. Johansson, U. W. Kirbach, D. M. Lee, M. Mendel, A. Nähler, V. Ninov, L. A. Omtvedt, J. B. Partin, G. Skarnemark, L. Stavsetra, R. Sudowe, N. Wiehl, B. Wierczinski, P. A. Wilk, P. M. Zielinski, J. V. Kratz, N. Trautmann, H. Nitsche, and D. C. Hoffman, J. Nucl. Radiochem. Sci. **3**, 121 (2002).
(6) L. Stavsetra, K. E. Gregorich, J. Alstad, H. Breivik, K. Eberhardt, C. M. Folden III, T. N. Ginter, M. Johansson, U. W. Kirbach, D. M. Lee, M. Mendel, L. A. Omtvedt, J. B. Patin, G. Skarnemark, R. Sudowe, P. A. Wilk, P. M. Zielinski, H. Nitsche, D. C. Hoffman, and J. P. Omtvedt, Nucl. Instrum. Methods A **543**, 509 (2005).
(7) Ch. E. Düllmann, G. K. Pang, C. M. Folden III, K. E. Gregorich, D. C. Hoffman, H. Nitsche, R. Sudowe, and P. M. Zielinski, *Advances in Nuclear and Radiochemistry, General and Interdisciplinary, Vol. 3*, Eds. S. M. Qaim and H. H. Coenen, Forschungszentrum Jülich GmbH, Jülich, (2004), p 147.
(8) Ch. E. Düllmann, C. M. Folden III, K. E. Gregorich, D. C.

Hoffman, D. Leitner, G. K. Pang, R. Sudowe, P. M. Zielinski, and H. Nitsche, Nucl. Instrum. Methods A **551**, 528 (2005).
(9) R. Sudowe, M. G. Galvert, Ch. E. Düllmann, L. M. Farina, C. M. Folden III, K. E. Gregorich, S. E. H. Gallaher, D. C. Hoffman, S. L. Nelson, D. C. Phillips, J. M. Schwantes, R. E. Wilson, P. M. Zielinski, and H. Nitsche, Radiochim. Acta **94**, 123 (2006).
(10) U. W. Kirbach, C. M. Folden III, T. N. Ginter, K. E. Gregorich, D. M. Lee, V. Ninov, J. P. Omtvedt, J. B. Patin, N. K. Seward, D. A. Strellis, R. Sudowe, A. Türler, P. A. Wilk, P. M. Zielinski, D. C. Hoffman, and H. Nitsche, Nucl. Instrum. Methods A **484**, 587 (2002).
(11) M. Schädel, J. Nucl. Radiochem. Sci. **8**, 47 (2007).
(12) H. Haba, D. Kaji, H. Kikunaga, T. Akiyama, N. Sato, K. Morimoto, A. Yoneda, K. Morita, T. Takabe, and A. Shinohara, J. Nucl. Radiochem. Sci. **8**, 55 (2007).
(13) H. Kikunaga, H. Haba, D. Kaji, and K. Morita, RIKEN Accel. Prog. Rep. **41** (in press).
(14) H. Haba, T. Akiyama, D. Kaji, H. Kikunaga, T. Kuribayashi, K. Morimoto, K. Morita, K. Ooe, N. Sato, A. Shinohara, T. Takabe, Y. Tashiro, A. Toyoshima, A. Yoneda, and T. Yoshimura, Eur. Phys. J. D **45**, 81 (2007).
(15) K. Morita, K. Morimoto, D. Kaji, H. Haba, E. Ideguchi, R. Kanungo, K. Katori, H. Koura, H. Kudo, T. Ohnishi, A. Ozawa, T. Suda, K. Sueki, I. Tanihata, H. Xu, A. V. Yeremin, A. Yoneda, A. Yoshida, Y.-L. Zhao, and T. Zhen, Eur. Phys. J. A **21**, 257 (2004).
(16) J. F. Ziegler, *The Stopping and Range of Ions in Matter, SRIM* (http://www.srim.org/).
(17) Y. Nagame, M. Asai, H. Haba, S. Goto, K. Tsukada, I. Nishinaka, K. Nishio, S. Ichikawa, A. Toyoshima, K. Akiyama, H. Nakahara, M. Sakama, M. Schädel, J. V. Kratz, H. W. Gäggeler, and A. Türler, J. Nucl. Radiochem. Sci. **3**, 85 (2002).
(18) R. B. Firestone and V. S. Shirley, *Table of Isotopes, 8th ed.* John Wiley & Sons, New York, (1996).
(19) G. N. Flerov, G. N. Akap'ev, A. G. Demin, V. A. Druin, Yu. V. Lobanov, and B. V. Fefilov, Sov. J. Nucl. Phys. **7**, 588 (1968).
(20) O. B. Tarasov and D. Bazin, *LISE++* (http://groups.nscl.msu.edu/lise/).